UNIVERSITEIT VAN PRETORIA
UNIVERSITY OF PRETORIA
YUNIBESITHI YA PRETORIA

# Rate and Yield Dependency of *Actinobacillus succinogenes* on Dissolved $CO_2$ Concentration

by

**Jolandi Herselman**

A dissertation submitted in partial fulfilment

of the requirements for the degree

**Master of Engineering (Chemical Engineering)**

in the

Department of Chemical Engineering

Faculty of Engineering, the Built Environment and Information Technology

University of Pretoria

Pretoria

**June 2016**

## Synopsis

Carbon dioxide serves as co-substrate in the production of succinic acid by *Actinobacillus succinogenes.* The transient concentration of dissolved $CO_2$ in the broth ($C_{CO_2}$) controls the uptake of $CO_2$ in the cell. Based on $C_{CO_2}$, three distinct regimes could be identified in which the behaviour of the organism differed with $C_{CO_2}$ availability. When $C_{CO_2}$ was higher than 8.4 mM (44.4% saturated at an atmospheric pressure of 86 kPa), there was no evidence of $CO_2$ limiting succinic acid productivity and flux to succinic acid remained constant. When $C_{CO_2}$ decreased below 8.4 mM a decrease in the succinic acid production and glucose consumption rates was observed to 28.01% and 19.89% of their original value respectively, at the lowest $C_{CO_2}$ value investigated. Below a $C_{CO_2}$ of 4 mM (21.16% saturated at an atmospheric pressure of 86 kPa), the productivity continued to decrease along with a shift in the total carbon flux from the succinic acid-producing pathway (C4-pathway) to the by-product-producing pathway (C3-pathway). The fraction of total carbon flux directed to the C4-pathway decreased from 0.48 to 0.33 at the lowest $C_{CO_2}$ value investigated. Although the by-product acetic acid concentration decreased to 88% of the original value, formic acid remained relatively stable and the ethanol concentration increased from an average of 0.26 $g.L^{-1}$ to 1 $g.L^{-1}$. The organism starts producing ethanol in order to satisfy the redox balance when the C4-pathway becomes less active. It was calculated that the flux shift to the C3-pathway does not favour ATP production. The organism is, however, still viable at the very low ATP production rates found at very low values of $C_{CO_2}$.

Since succinic acid production is not limited at relatively low values of $C_{CO_2}$ (44.4% saturation), adequate $CO_2$ supply to the fermenter can be achieved without major $CO_2$ sparging which is beneficial from an industrial processing perspective.

**Keywords:** $CO_2$ limitations, *Actinobacillus succinogenes,* mass transfer coefficient, metabolite distribution, productivity

## Acknowledgements

Thanks to Prof. Willie Nicol for his financial support for this research and for the excellent role he played as supervisor.

The financial assistance of the National Research Foundation (NRF) towards this research is gratefully acknowledged. Opinions expressed and conclusions arrived at are those of the author and are not necessarily to be attributed to the NRF.

The financial assistance of the Sugar Milling Research Institute via the Step-Bio Project is hereby gratefully acknowledged.

# Contents

# List of Figures

# List of Tables

## Nomenclature

| | | |
|---|---|---|
| $A_E$ | Surface area of cell | $m^2$ |
| $\alpha_G$ | Bunsen coefficient for $CO_2$ in a medium | |
| $\alpha_{G,0}$ | Bunsen coefficient for $CO_2$ in a pure solvent | |
| $b_n$ | Organic substance-specific parameter of Rischbieter | $m^3.kg^{-1}$ |
| $b_{G,0;}\ b_{G,T}$ | Gas-specific parameter of Rischbieter | $m3.kg^{-1}$ |
| $C_{CO_2}$ | Dissolved $CO_2$ concentration in the bulk | $mol.L^{-1}$ |
| $C^*_{CO_2}(l)$ | $CO_2$ liquid concentration in equilibrium with the gas phase | $mol.L^{-1}$ |
| $C^{eq}_{CO_2}$ | $CO_2$ concentration at equilibrium conditions | $mol.L^{-1}$ |
| $C^{eq}_{CO_3^{2-}}$ | Carbonate concentration at equilibrium conditions | $mol.L^{-1}$ |
| $C^{eq}_{CO_{2t}}$ | $CO_2$ concentration inside the cell at equilibrium | $mol.L^{-1}$ |
| $C^{eq}_{HCO_3^-t}$ | $HCO_3^-$ concentration inside the cell at equilibrium conditions | $mol.L^{-1}$ |
| $C^{eq}_{H_2CO_3t}$ | $H_2CO_3$ concentration inside the cell at equilibrium conditions | $mol.L^{-1}$ |
| $C_{GL,\ eff}$ | Effective glucose concentration in medium | $g.L^{-1}$ |
| $C_{GL,\ feed}$ | Glucose concentration in feed | $g.L^{-1}$ |
| $C^{eq}_{H^+}$ | Hydronium ion concentration at equilibrium conditions | $mol.L^{-1}$ |
| $C^{eq}_{HCO_3^-}$ | $HCO_3^-$ concentration at equilibrium | |

| | | |
|---|---|---|
| | conditions | $mol.L^{-1}$ |
| $C^{eq}_{H_2CO_3}$ | $H_2CO_3$ concentration at equilibrium conditions | $mol.L^{-1}$ |
| $c_i$ | Concentration of ion i species | $mol.L^{-1}$ |
| $c_{n,j}$ | Organic substrate j species | $kg.m^{-3}$ |
| $C_{AA}$ | Acetic acid concentration | $g.L^{-1}$ |
| $C_{ETH}$ | Ethanol concentration | $g.L^{-1}$ |
| $C_{FA}$ | Formic acid concentration | $g.L^{-1}$ |
| $C_{PYR}$ | Pyruvic acid concentration | $g.L^{-1}$ |
| $C_{SA}$ | Succinic acid concentration | $g.L^{-1}$ |
| $C_T$ | Total carbonate concentration | $mol.L^{-1}$ |
| $C_x$ | Concentration of biomass | $g.L^{-1}$ |
| $C_{OH}$ | Molar concentration of sodium hydroxide | $mol.L^{-1}$ |
| $C^{feed}_{H^+}$ | Hydronium ion concentration at feed pH | $mol.L^{-1}$ |
| $C_{H^+}$ | Hydronium ion concentration in the medium | $mol.L^{-1}$ |
| $C^{P}_{CO_2}$ | Critical $CO_2$ concentration for productivity | mM |
| $C^{Y}_{CO_2}$ | Critical $CO_2$ concentration for flux | mM |
| $D$ | Dilution | $h^{-1}$ |
| $f_4$ | Fraction of total carbon flux entering the C4-pathway | |
| $H_0$ | Henry's constant in pure water at 37 ºC | $kPa.L.mol^{-1}$ |
| $H$ | Henry's constant for $CO_2$ in medium | $kPa.L.mol^{-1}$ |
| $h_{G,0;}\ h_{G,T}$ | Gas-specific parameter of Weisenberger and Schumpe model | $mol.L^{-1}$ |

| | | |
|---|---|---|
| $h_i$ | Ion-specific parameter of the Weisenberger and Schumpe model | $L.mol^{-1}$ |
| $J_{CO2}$ | Diffusion rate through cell | $mol.s^{-1}$ |
| $K_1$ | Equilibrium dissociation constant | |
| $K_2$ | Equilibrium dissociation constant | $mol.L^{-1}$ |
| $K_3$ | Equilibrium dissociation constant | $mol.L^{-1}$ |
| $K_4$ | Equilibrium dissociation constant | $mol.L^{-1}$ |
| $k_g a_g$ | Mass transfer coefficient | $h^{-1}$ |
| $K_M$ | Michaelis Menten constant | $mol.L^{-1}$ or $mmol.L^{-1}$ |
| $K_{n,j}$ | Organic substrate-specific parameter of Weisenberger and Schumpe model | $m^3.kg^{-1}$ |
| $P$ | Permeability coefficient | $m.s^{-1}$ |
| $P_{CO2}$ | Partial pressure of $CO_2$ | kPa |
| $P_p$ | Rate of proton production | $mol.L^{-1}.h^{-1}$ |
| $q_{GLC}$ | Rate of glucose consumption | $mol.L^{-1}.h^{-1}$ |
| $P_{SA}$ | Succinic acid productivity | $g.L^{-1}.h^{-1}$ |
| $Q$ | Total flow rate into reactor | $mL.h^{-1}$ |
| $Q_D$ | NaOH dosing flow rate | $mL.h^{-1}$ |
| $Q_{feed}$ | Flow rate of fresh feed into reactor | $mL.h^{-1}$ |
| $r_A$ | Gas-to-liquid mass transfer volumetric rate | $mol.L^{-1}.h^{-1}$ |
| $r_{CO_2}$ | Rate of $CO_2$ consumption | $mol.L^{-1}.h^{-1}$ |
| $V_{max}$ | Maximal reaction rate | $mol.L^{-1}.h^{-1}$ |
| $V$ | Volume | mL |
| $vvm$ | Volumetric flow rate of gas per reactor volume | $min^{-1}$ |
| $Y_{GLSA}$ | Yield of succinic acid over glucose | $g.g^{-1}$ |

| | | |
|---|---|---|
| $Y_{AASA}$ | Yield of succinic acid over acetic acid | $g.g^{-1}$ |
| $Y_{AAFA}$ | Yield of formic acid over acetic acid | $g.g^{-1}$ |
| $Y_{XSA}$ | Yield of succinic acid over biomass | $g.g^{-1}$ |
| $Y_{SATP}$ | Molar yield of ATP over glucose | $mol.mol^{-1}$ |
| $Y_{SE}$ | Molar yield of ethanol over glucose | $mol.mol^{-1}$ |

# 1 Introduction

It is a well-known fact that the Earth's fossil fuel supply has been dwindling in recent times and that there is a need to find methods of producing alternatives to petroleum-based products and to replace the petroleum industry as a whole. In the petroleum refinery a few basic raw materials (petroleum, natural gas and $O_2$ + $N_2$ from the atmosphere) are used to produce platform chemicals (such as ethyl benzene, iso-butylene and butadiene) which are turned into secondary chemicals (such as styrene, adipic acid and acetone). These are used to produce intermediates and then consumer goods for a large number of industries. Biorefining is a possible alternative to petroleum refining. Currently there is a global research effort under way into the potential of biorefineries where sugars (starch-based and lignocellulosic) are converted into the same important chemicals and intermediates obtained in the petroleum-based refinery but by using microbes or enzymes.

Succinic acid has been recognised for some time by researchers as a top chemical that can be produced from biorefinery carbohydrates (Werpy & Petersen, 2004; Bozell & Petersen, 2010). Bio-succinic acid is already being produced on an industrial scale by several companies, and there are plans for plants to come online in the future. Companies such as Reverdia (10 000 $t.a^{-1}$) and Myriant (201 210 $t.a^{-1}$), along with joint ventures between BASF and Purac (75 000 $t.a^{-1}$) and BioAmber and Mitsui (164 000 $t.a^{-1}$) are at the forefront of production of bio-succinic acid (ICIS Chemical Business, 2012). Succinic acid is used to produce a variety of bio-based products for the agricultural, food, chemical and pharmaceutical industries. Some of the products produced from succinic acid that are receiving increased interest are biodegradable polymers (polybutylene succinate (PBS)), solvents (butanediol (BDO)) and polyester polyols which can be used to produce coatings, adhesives, sealants and elastomers (ICIS Chemical Business, 2012; Stepan, 2012). The bio-succinic market was estimated to have a value of $115.2 million in 2013, and is expected to grow to $1.1 billion by 2020 (Allied Market Research, 2014).

To date a number of succinic acid-producing microorganisms have been identified. The most promising of these are *Actinobacillus succinogenes* (Guettler, Rumler & Jain, 1999), *Mannheimia succiniciproducens* (Lee *et al.,* 2002), *Anaerobiospirillum*

*succiniciproducens* (Lee *et al.,* 2000) and *Escherichia coli* (Lin, Bennett & San, 2004). *A.succinogenes* is proving to be promising in commercial production due to its ability to use a wide variety of substrates (Almqvist *et al.,* 2016), produce succinate in high concentrations (Zeikus, Jain & Elankovan, 1999), tolerate highly acidic conditions (Lin *et al.,* 2008) and naturally form biofilms (Urbance *et al*., 2003), thereby increasing the productivity of the system.

The term biorefinery refers to the integration of a range of biomass conversion processes to produce not only different types of chemicals, but also fuel and electrical power from biomass (Cherubini, 2010). This fuel and electrical power will most likely be reused by the plant. One example of efficient biorefinery integration is when ethanol and succinate fermentations are combined: 2 mol waste $CO_2$/mol glucose is formed during ethanol fermentation (Zeikus *et al*., 1999; Urbance *et al.,* 2004) while succinate fermentation consumes $CO_2$. Integration of these two processes would decrease carbon loss in the form of waste $CO_2$. Another example of efficient biorefinery integration was demonstrated by Gunnarson, Alvarado-Morales and Angelidaki (2014), who were able to upgrade biogas, an attractive renewable energy carrier, containing 50-75% $CH_4$ and 25-50% $CO_2$ to a purity of up to 95% $CH_4$ by using the $CO_2$ as an inorganic carbon source in a fermentation with *A. succinogenes*, thereby increasing the energy content of the biogas. The removed $CO_2$ would typically be released into the atmosphere since the technologies for $CO_2$ capturing and storing are costly. It is expected that processes using $CO_2$ as raw material will become increasingly important (Aresta, Dibenedetto & Angelini, 2014).

Fundamental process development work is required to assist in the upscaling and economic feasibility of the biorefinery. One area for optimisation of succinic acid production via fermentation is the $CO_2$ delivery rate to the cell. It therefore comes as no surprise that the $CO_2$ supply in succinic acid production appears in the earliest publications on *A. succinogenes* (Van der Werf *et al.*, 1997). Diffusion of dissolved $CO_2$ across the membrane is the main transport mechanism of inorganic carbon supply to the cell since $HCO_3^-$ permeation through the lipid membrane is negligible (Lu, Eiteman & Altman, 2009; Zou *et al.,* 2011). The $CO_2$ supply in succinic acid fermentation is therefore best studied by monitoring the $CO_2$ concentration in the fermentation broth ($C_{CO_2}$). This variable will decrease if the rate of $CO_2$ uptake by the

cell exceeds the rate of $CO_2$ supply to the broth. Quantification of the required inorganic carbon source will prevent excessive and expensive sparging during bio-succinic production. $CO_2$ can either be supplied via gas-liquid mass transfer or by adding highly insoluble carbonate salts, such as $MgCO_3$ and $CaCO_3$, to the fermentation medium. Whereas gaseous $CO_2$ is readily available at the plant, the use of salts would lead to extra expenditure.

It is well proven in the literature that the $CO_2$ supply alters the productivity and catabolic product distribution of *A. succinogenes* (Van der Werf *et al.,* 1997; Zou *et al.,* 2011; Xi *et al.,* 2011; Gunnarson *et al.,* 2014). However, all the studies used batch fermentations, in which the initial carbonate salt concentration and $CO_2$ partial pressure were varied. The instantaneous succinic acid productivity varies appreciably during a batch run (Corona-González, Bories, González-Álvarez & Pelayo-Ortiz, 2008; Lin *et al.*, 2008), and within high-productivity phases the dissolved $CO_2$ concentration can drop below saturation if the gas-liquid mass transfer is rate controlling and when the carbonates are supplied in concentrations less than the stoichiometric amount. This can limit batch fermentations, leading to lower final values for productivity and yield. A continuous mode of operation allows a steady state analysis of the effect of $CO_2$. At a steady state the $C_{CO_2}$ concentration will remain constant and therefore the true effect on the productivity and yield of *A. succinogenes* can be observed. For gaseous $CO_2$ the gas-liquid mass transfer will determine whether a sufficient supply of $CO_2$ is maintained. The maximum $C_{CO_2}$ value is determined by the partial pressure of the $CO_2$ in the gas phase, which is in the vicinity of 20 mM (Zou *et al.,* 2011; Xi *et al*., 2011; Gunnarson e*t al*., 2014). For the carbonate supply the influence of mixing on the solid dissolution rate will determine whether enough $CO_2$ can be supplied. Both these routes require proper understanding and quantification of the effect of $C_{CO_2}$ on succinic acid yield and cell-based productivity. To date no study has investigated these crucial relationships.

The shortcoming mentioned above in the literature on *A. succinogenes* fermentation is addressed in this study. The authors have opted for a steady state analysis of the fermentation in order to maintain $C_{CO_2}$ at a stable value. Accurate gas-liquid mass transfer measurements were used to calculate $C_{CO_2}$ at various steady state conditions. Continuous fermentation of *A. succinogenes* with standard complex-medium

formulations will inevitably result in biofilm formation. Therefore an effort was made to control the immobilised amount of biomass by operating at close to full conversion of the substrate glucose. Mass balance checks were performed to ensure that all the major metabolites were detected.

# 2 Literature

## 2.1 Bio-succinic acid

Succinic acid (SA) is a four-carbon dicarboxylic acid intermediate in the TCA cycle. The structure of succinic acid is shown in Figure 2-1.

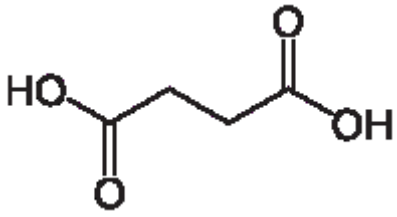


***Figure 2-1:*** *Molecular structure of succinic acid*

BASF states that in 2012 the demand for succinic acid was 30 000 – 35 000 $t.a^{-1}$ and that double-digit growth rates are expected up to 2017 (ICIS Chemical Business, 2012). Succinic acid is traditionally produced through the catalytic hydrogenation of maleic acid from n-butane (Trivedi & Culbertson, 1982). The availability of petroleum-based succinic acid is limited due to volatility of the fossil fuel prices and the high carbon footprint. The need for sustainable solutions, products with an improved environmental impact, and biodegradable and bio-based products have led to the biological manufacturing of succinic acid. The bio-succinic market was estimated to have a value of $115.2 million in 2013 and is expected to grow to $1.1 billion by 2020 (Allied Market Research, 2014).

The cost of maleic anhydride contributes significantly to production costs of petroleum-based succinic acid (Trivedi & Culbertson, 1982). The selling price of US maleic anhydride ranged between $\$1.54.kg^{-1}$ and $\$1.8.kg^{-1}$ in 2014 and the first part of 2015 (Na, 2015). As mentioned, the bio-based production of succinic acid involves the use of sugars (glucose and C5-sugars) and $CO_2$ as substrates. These sugars can be obtained from sugar-rich side streams that are produced, for example, in the agricultural or paper and pulp industries, which up to now have mostly been burnt for energy production. These sugars would be far more valuable when extracted or used, as is, as a carbon source in fermentations to produce valuable chemical intermediates. This raw material is therefore a cheaper option. Even the price of glucose with a high purity ranges between $\$0.45.kg^{-1}$ and $\$0.465.kg^{-1}$ (Alibaba, 2016). This is a lot lower

than the price of maleic anhydride. The biological production of succinic acid has the added benefit of consuming 1 mol of $CO_2$ per mole of succinic acid produced, in contrast to the traditional hydrogenation that produces $CO_2$.

Succinic acid has been recognised as one of the top chemical opportunities that can be produced from biorefinery carbohydrates (Werpy & Petersen, 2004; Bozell & Petersen, 2010). One of the selection criteria that Bozell and Petersen (2010) employed was whether scale-up of the product or technology is under way. Some key players already have pilot and commercial plants in operation producing bio-succinic acid. Table 2-1 shows the bio-production capacity of planned and current commercial plants. By 2015 new bio-succinic acid plants expected to have come on stream were expected to have a capacity in excess of 200 000 $t.a^{-1}$ (ICIS Chemical Business, 2012).

***Table 2-1**: Bio-production capacity of succinic acid (ICIS Chemical Business, 2012)*

| Company | Annual capacity | Plant Location | Operational date |
|---|---|---|---|
| BASF-Purac JV | 50 000 tons | TBA | TBA |
| BASF-Purac JV | 25 000 tons | Barcelona, Spain | 2013 |
| BioAmber-ARD | 3 000 tons capacity | Pomacle, France | Full capacity by Q2 2012 |
| BioAmber-Mitsui JV | 65 000 tons | TBA (USA or Brazil) | TBA |
| BioAmber-Mitsui JV | 17 000 tons (initial) 34 000 tons (full capacity) | Sarnia, Ontario, Canada | 2013 |
| BioAmber-Mitsui JV | 65 000 tons | Thailand | 2014 |
| Myriant | 13 600 tons | Lake Providence, Louisiana | Q1 2013 |
| Myriant-China National Blue Star | 110 000 tons | Nanjing, China | TBA |
| Myriant | 77 110 tons | Lake Providence, Louisiana | Q1 2014 |
| Myriant-Uhde (owner and operator) | 500 tons (first year) | Infraleuna site, Germany | H1 2012 |
| Reverdia (DSM-Roquette) | 10 000 tons | Cassano Spinola, Italy | H2 2012 |

Succinic acid's potential as a platform chemical to be used in the production of various bio-based products is another criterion which Bozell and Petersen (2010) used to determine their list of top chemical opportunities from biorefinery carbohydrates. One such bio-based product is polybutylene succinate (PBS). PBS is produced by combining succinic acid and 1,4 butanediol. BASF is working on a modified PBS with higher heat distortion tolerance, greater strength and lower cost. PBS can also be combined with polymers (polypropylene, polystyrene and polycarbonate) or polylactic acid (polyhydroxyalkanoate and poly-3-hydroxy butyrate co-valerate). These PBS composites can be combined with fibres or fillers for use in automotive interiors, non-wovens, construction material and consumer goods. The current petro-derived market is 5 000 – 6 000 tons.year$^{-1}$ and is expected to increase to 50 000 tons.year$^{-1}$ by 2017 and 100 000 tons.year$^{-1}$ by 2022 according to Mitsubishi Chemical's petrochemical research and development division (ICIS Chemical Business, 2012). Another bio-based product, produced from succinic acid, is butanediol (BDO). The market for BDO is 2 000 000 tons.year$^{-1}$, of which 1 000 000 tons.year$^{-1}$ is used to produce tetrahydrofuran (THF), an intermediate in the production of elastic fibres and engineering thermoplastic polybutylene terephthalate (PBT) (ICIS Chemical Business, 2012). In 2010 BioAmber licensed its US-based Du Pont's hydrogenation catalyst technology to make bio-BDO and bio-THF from bio-succinic acid (ICIS Chemical Business, 2012). They expected the market for BDO and THF to exceed $4bn (ICIS Chemical Business, 2012). A third product manufactured from succinic acid is polyester polyols for polyurethanes. According to Reverdia (2015), succinic acid will replace petroleum-based adipic acid for the production of improved polyurethane. Polyurethanes are used for adhesives for hot-melt applications, coatings, sealants, elastomers for artificial leather applications, etc. Other products produced with succinic acid include plasticisers (PVC pipes, engineered plastics, toys), coatings and polymers and esters (adhesives, sealants, electrical tape) (Myriant, 2016).

To date a number of succinic acid-producing microorganisms have been identified. The most promising of these include *Actinobacillus succinogenes* (Guettler *et al.,* 1999), *Mannheimia succiniciproducens* (Lee *et al.,* 2002), *Anaerobiospirillum succiniciproducens* (Lee *et al.,* 2000) and *Escherichia coli* (Lin *et al*., 2004).

*A. succinogenes* is proving to be promising in commercial production due to its ability to use a wide variety of substrates, produce succinate in high concentrations (Zeikus

*et al.*, 1999) and its high tolerance to acids (Lin *et al.,* 2008). *A. succinogenes* was isolated from the bovine rumen. It is a mesophilic, facultatively anaerobic, pleomorphic, Gram-negative rod bacteria. *A. succinogenes* is a capnophilic, osmotolerant succinogen (Guettler *et al.,* 1999; McKinlay, Zeikus & Vieille, 2005) showing fairly constant product ratios between a pH of 6 – 7.4 (Van der Werf *et al.,* 1997).

## 2.2 Metabolic pathway of *A. succinogenes*

Figure 2-2 shows the central metabolic network of *A. succinogenes.* It converts glucose to phosphoenolpyruvate (PEP) through glycolysis using the Embden-Meyerhof-Parnas (EMP) pathway. From PEP the metabolism splits into the following two branches: i) the formate-, acetate and ethanol-producing C3 branches and ii) the succinate-producing C4 branch.

In the C4-pathway the enzyme phosphoenolpyruvate carboxykinase (PCK) catalyses the formation of oxaloacetate from the reversible carboxylation of PEP. This reaction produces one ATP molecule for every PEP molecule converted. Oxaloacetate is then converted in the reductive TCA cycle to malate by the enzyme malate dehydrogenase. One mole of NADH is consumed. Malate is converted to fumarate by the enzyme fumarase. Fumarate is then converted to succinic acid with the consumption of 1 mole of NADH by the enzyme fumarate reductase, $\frac{2}{3}$ mole of ATP is also produced when fumarate is converted to succinic acid (McKinlay *et al*., 2009).

In the C3-pathway PEP is converted to pyruvate with the production of one molecule of ATP by the enzyme pyruvate kinase. Pyruvate can then be converted by two possible routes. The first is the pyruvate dehydrogenase route and the second the pyruvate formate-lyase pathway in which formate is formed. The pyruvate dehydrogenase pathway leads to the formation of 1 mole of NADH and 1 mole of $CO_2$. By performing redox balances on the system, the yield of products can be calculated for the case in which the pyruvate dehydrogenase pathway is active while the pyruvate formate-lyase pathway is inactive. Theoretically it can be shown that this scenario will give a maximum value for the yield of succinic acid over acetic acid ($Y_{AASA}$) equal to 3.93 $g.g^{-1}$ (2 $mol.mol^{-1}$) and a maximum value for the yield of succinic acid on glucose ($Y_{GLSA}$) of 0.87 $g.g^{-1}$ (Bradfield & Nicol, 2014). If pyruvate is converted solely through the pyruvate formate-lyase pathway, the two major by-products acetate ($C_{AA}$) and

formate ($C_{FA}$) (ethanol concentrations are usually negligible) will be produced in equimolar amounts since the acetyl-coA molecule formed from pyruvate is directly converted to acetic acid. In this case the yield of acetic acid over formic acid ($Y_{AAFA}$) will be equal to 0.77 $g.g^{-1}$, the maximum value for $Y_{AASA}$ will be equal to 1.97 $g.g^{-1}$ and the maximum for $Y_{GLSA}$ will be 0.66 $g.g^{-1}$ in the event of no biomass formation (Bradfield & Nicol, 2014). The formate produced in the pyruvate formate-lyase pathway can be converted to $CO_2$ and NADH if the enzyme formate dehydrogenase is present. For this case, $Y_{AASA}$ will also give a value equal to 3.93 $g.g^{-1}$ (Bradfield & Nicol, 2014). If formate dehydrogenase is present in combination with pyruvate formate-lyase, the same amount of NADH gain as in the pyruvate dehydrogenase pathway can be achieved.

Acetyl-CoA is the branch point for acetate and ethanol formation. Acetyl-coA is converted to acetate with the formation of one mole of ATP using the enzyme acetate kinase. For ethanol formation, acetyl-CoA is first converted to acetaldehyde with the consumption of one mole of NADH using the enzyme acetaldehyde dehydrogenase. The acetaldehyde is then converted to ethanol with the enzyme alcohol dehydrogenase, which also leads to the consumption of 1 mole of NADH.

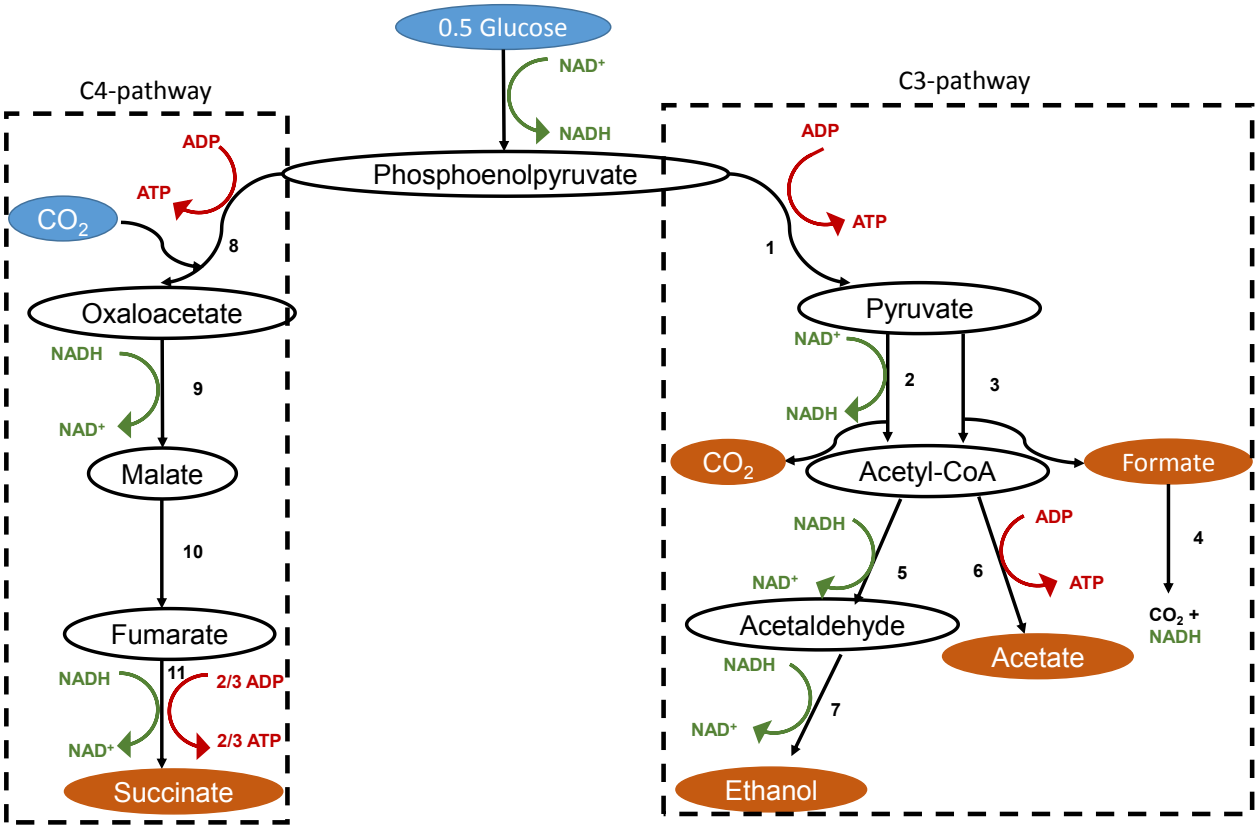


***Figure 2-2**: Simplified metabolic network of A. succinogenes showing the pathways leading to major metabolites (McKinlay et al., 2007). Glycolysis occurs through the Embden-Meyerhof-Parnas (EMP) pathway (details not shown). (1) pyruvate kinase , (2) pyruvate dehydrogenase, (3) pyruvate formate-lyase, (4) formate dehydrogenase, (5) alcohol dehydrogenase, (6) acetate kinase, (7) acetaldehyde dehydrogenase (8) phosphoenolpyruvate carboxykinase, (9) malate dehydrogenase, (10) fumarase, (11) fumarate reductase*

As can be seen from Figure 2-2, 1 mol $CO_2$ is theoretically required for the synthesis of 1 mol succinic acid, therefore $CO_2$ should play an important role in succinic acid production (Van der Werf *et al.*, 1997). As mentioned before, the enzyme responsible for $CO_2$ fixation in *A. succinogenes* is phosphoenolpyruvate carboxykinase.

## 2.3 Phosphoenolpyruvate carboxykinase

Phosphoenolpyruvate carboxykinase (PCK) catalyses the formation of oxaloacetate (OAA) from the reversible carboxylation of phosphoenolpyruvate (PEP) and the naturally accompanying phosphorylation of adenosine diphosphate (ADP) to adenosine triphosphate (ATP) (McKinlay *et al.*, 2007). This reaction is given in Equation (2-1).

$$PEP + ADP + CO_2 \leftrightarrow OAA + ATP \quad \textbf{(2-1)}$$

PCK exhibited Michaelis Menten kinetics. The kinetic features of PCK were obtained by using a Lineweaver-Burk plot of specific activities at various substrate concentrations. The apparent $K_M$ values for PEP, $HCO_3^-$ and ADP were 0.54 mM, 17 mM and 0.42 mM respectively (Podkovyrov and Zeikus, 1993). The apparent $V_{max}$ value was 10 U (mg protein)$^{-1}$ (Podkovyrov and Zeikus, 1993). The apparent $K_M$ values for OAA and ATP were 1.2 mM and 2.3 mM respectively (Podkovyrov and Zeikus, 1993). No activity was observed when inosine or guanosine nucleotides (GDP) were used in place of ADP. This specificity for ADP was typical of PCKs from bacterial species. Van der Werf *et al*. (1997) found that the flux of PEP in either pathway of *Actinobacillus* sp.130Z is not influenced by the enzyme levels of the PEP-converting enzymes since both enzymes are constitutive. The in vivo activity of these enzymes is determined by the intracellular concentration of the different substrate of these enzymes.

Samuelov *et al*. (1991) analysed the influence of $CO_2$ and $HCO_3^-$ on enzyme levels in *A. succiniciproducens*, which also uses the enzyme PEP caboxykinase. The system was supplied with 1.5 g.L$^{-1}$ $Na_2CO_3$ and 4.7 g.L$^{-1}$ $Na_2CO_3$ with continuous sparging of $CO_2$ at 1 L.min$^{-1}$ in order to create a low and high $CO_2$-$HCO_3^-$ environment respectively. The PEP carboxykinase level increased by up to 35.6 times when comparing low to excess $CO_2$ and $HCO_3^-$ growth conditions.

Podkovyrov and Zeikus (1993) found that the optimum pH for PCK in *A. succiniciproducens* was between 6.5 and 7.1. The enzyme was stable in the pH range 5.0 – 9.0, losing activity at pH values lower than 4.5 and retaining some activity in the pH range 9 – 12. pH does not necessarily affect the dissolved $CO_2$ concentration, but it does influence the total carbon concentration ($C_T$). As discussed in Section 2.5.3 $CO_2$ in the broth is in equilibrium with $HCO_3^-$ and $CO_3^{2-}$ which is also produced when $CO_2$ reacts with water. $C_T$ is the sum of the molar amount of $CO_2$, $HCO_3^-$ and $CO_3^{2-}$ in the fermentation broth. The highest $C_T$ value was obtained at a pH value of 7.4; however, the key enzyme that fixed $CO_2$, synthesised at pH 7.4, was not suitable. The external medium pH affects the cytoplasmic pH, which may determine the PCK

activity. Samuelov (referred by Xi *et al.,* 2011) reported that the activity of PEP carboxylase kinase at pH 6.2 was 35 times greater than at pH 7.4 in *A. succiniciproducens.* In contrast Xi *et al. (*2011) found that the activity of pyruvic acid kinase (PYK), which is responsible for the production of formic acid, acetic acid and other by-products, increased with increasing pH.

### 2.4 Performance studies of *A. succinogenes*

Several continuous, fed batch and batch studies have been performed using *A. succinogenes* 130Z and glucose as a substrate.

Table 2-2 is a summary of the highest yields and productivities achieved to date in a continuous reactor setup. Only results obtained under conditions similar to those used in this study are presented. These conditions include pH, temperature, medium composition, neutralisation agent and conditions of $CO_2$ saturation. The data for maximum yield, titre and productivity given for each study may not have been obtained in the same fermentation or at exactly the same conditions. The highest succinic acid titre and productivity obtained in a continuous study is 48.5 $g.L^{-1}$ (Bradfield & Nicol, 2014) and 17.1 $g.L^{-1}.h^{-1}$ (Brink & Nicol, 2014) respectively. The highest succinic acid yield ($Y_{GLSA}$) obtained is 0.91 $g.g^{-1}$, while the highest $Y_{AASA}$ value is equal to 5.7 $g.g^{-1}$ (Bradfield & Nicol, 2014). Bradfield & Nicol (2014) reported that the $Y_{AAFA}$ decreased to zero with an increase in the glucose consumption rate, suggesting an increase in dehydrogenase activity. The highest yield and productivities obtained in batch, fed batch and repeat batch runs are given in Table 2-3. The highest succinic acid titre and productivity obtained in a batch study is equal to 79 $g.L^{-1}$ (Guettler, Jain & Soni, 1998) and 1.45 $g.L^{-1}.h^{-1}$ (Bradfield, *et al.*, 2015) respectively. The highest $Y_{GLSA}$ is equal to 0.92 $g.g^{-1}$ (Urbance *et al*., 2003), while the highest value of $Y_{AASA}$ is equal to 5.6 $g.g^{-1}$ (Guettler, Jain & Rumler, 1996). The lowest $Y_{AAFA}$ value reported in literature is equal to 0.38 $g.g^{-1}$ (Lin *et al.,* 2008).

***Table 2-2**: Continuous fermentation studies performed using* A. succinogenes *130Z at a pH of around 6.8 and a temperature of 37 ˚C in an undefined medium using NaOH as a neutralising agent at $CO_2$-saturated conditions*

| Author | Medium | $C_{SA}$ ($g.L^{-1}$) | $C_{ETH}$ ($g.L^{-1}$) | $Y_{GLSA}$ ($g.g^{-1}$) | $Y_{AASA}$ ($g.g^{-1}$) | $Y_{AAFA}$ ($g.g^{-1}$) | $P_{SA}$ ($g.L^{-1}.h^{-1}$) |
|---|---|---|---|---|---|---|---|
| Van Heerden & Nicol, 2014 | YE; CSL | 13 | 0.08 | 0.71 | 2.5 | 0.77 | 6.35 |
| Urbance *et al*., 2004 | YE; CSL | 10.4 | - | 0.76 | - | - | 8.8 |
| Bradfield & Nicol, 2014 | YE; CSL | 48.5 | - | 0.91 | 5.7 | 0.77 | - |
| Kim *et al*., 2009 | YE | 18.2 | - | 0.58 | 2.77 | 0.78 | 6.63 |
| Maharaj, Bradfield & Nicol, 2014 | YE; CSL | 32.5 | - | 0.9 | 4.8 | 0.1 | 10.8 |
| Brink & Nicol, 2014* | YE; CSL | 7.14 | - | 0.61 | 1.55 | 0.73 | 1.83 |
| Brink & Nicol, 2014 | YE; CSL | 18.16 | - | 0.75 | 3.3 | 0.8 | 17.1 |

* Chemostat operation, YE = yeast extract, CSL = corn steep liquor

***Table 2-3:*** *Batch studies performed using* A. succinogenes *130Z at a pH of around 6.8 and a temperature of 37 ˚C in an undefined medium using NaOH as a neutralising agent at $CO_2$-saturated conditions*

| Author | Medium | Operation mode | $C_{SA}$ ($g.L^{-1}$) | $C_{ETH}$ ($g.L^{-1}$) | $Y_{GLSA}$ ($g.g^{-1}$) | $Y_{AASA}$ ($g.g^{-1}$) | $Y_{AAFA}$ ($g.g^{-1}$) | $P_{SA}$ ($g.L^{-1}.h^{-1}$) |
|---|---|---|---|---|---|---|---|---|
| Urbance *et al*., 2004 | YE; CSL | Repeat batch | 35.1 | - | 0.87 | - | - | 0.9 |
| Lin *et al*., 2008 | YE (Semi-defined medium) | Batch | 47.6 | - | 0.78 | 5.34 | 0.38 | - |
| Corona-González *et al*., 208 | YE | Batch | 33.8 | - | 0.62 | 5.2 | 0.81 | 1.37 |
| Guettler, Jain & Rumler, 1996 [i] | YE; CSL | Batch | 67.2 | - | 0..68 | 5.6 | 0.73 | - |
| Guettler *et al*., 1998 | YE; CSL | Batch | 79 | - | 0.79 | - | - | - |
| Urbance *et al.,* 2003 (Medium tests) | YE: CSL | Batch | 14 | - | 0.7 | - | - | - |
| Urbance *et al.,* 2003 (Plastic composite support tests) | YE; CSL | Batch | 9.4 | - | 0.92 | - | - | - |
| Bradfield *et al.,* 2015 | YE;CSL | Batch | 48 | - | 0.72 | - | - | 1.45 |
| Almqvist *et al.,* 2016 | YE | Batch | - | - | 0.59 | - | - | 0.7 |

YE = Yeast Extract, CSL = Corn Steep liquor

## 2.5 Carbon dioxide availability model

Gaseous $CO_2$ must undergo a few mass transfer and reaction steps before it can attach to the enzyme-active site and take part in the $CO_2$ fixing reaction as shown by Equation (2-1). Figure 2-3 illustrates the processes that need to be completed before attachment can occur, and the $CO_2$ concentration profile.

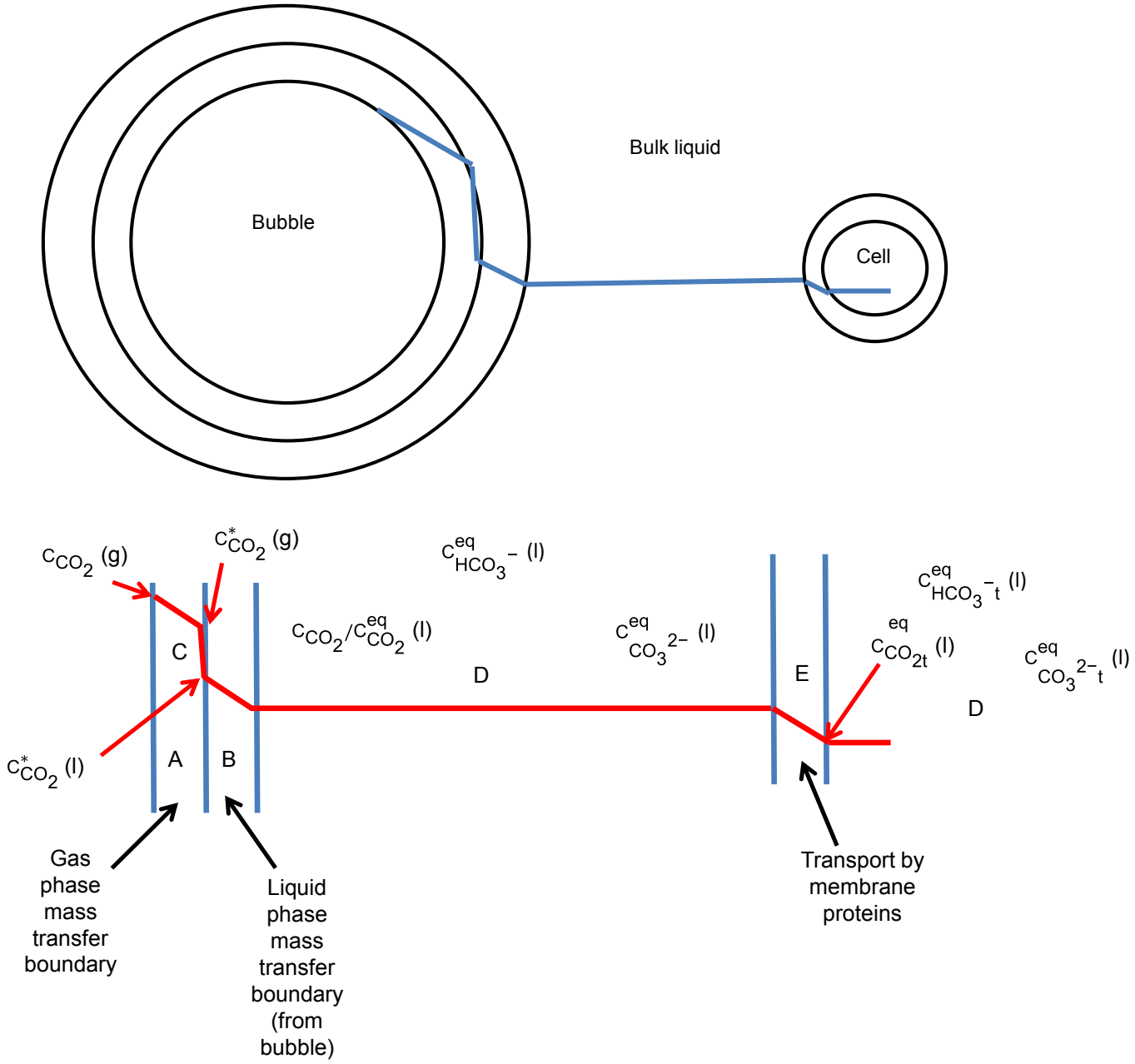


***Figure 2-3**: Gaseous $CO_2$ transfer process from bubble to enzyme*

In this study gaseous $CO_2$ is added directly to the recycle line and then passes through a distributor plate in order to break the gas up into smaller bubbles. The first step which the gas undergoes when coming into contact with the fermentation medium is gas-to-

liquid mass transfer. This step is discussed in Section 2.5.1. This mass transfer step is dependent on the phase equilibrium that exists between the gas and liquid phases, and is discussed in Section 2.5.2. After the $CO_2$ dissolution several equilibrium reactions take place as discussed in Section 2.5.3. At the cell surface certain transport membrane proteins need to be present to carry the substrate into the cell (Section 2.5.4), after which the substrate can bind to the enzyme-active site and react as discussed in Section 2.3.

### 2.5.1 Gas-to-liquid mass transfer (labelled A and B in Figure 2-3)

The gas side liquid-mass transfer step (labelled A in Figure 2-3) can usually be ignored since this process is so fast that the $CO_2$ concentration gradient remains the same. The liquid side gas-liquid mass transfer volumetric rate (labelled B in Figure 2-3) is given by Equation (2-2) (Cussler, 1997:218).

$$-r_A = k_g a_g (C^*_{CO_2}(l) - C_{CO_2}) \quad \textbf{(2-2)}$$

In Equation (2-2) $k_g a_g$ is the mass transfer coefficient, which gives a measure of the efficiency of $CO_2$ transfer in units of $h^{-1}$. $C^*_{CO_2}(l)$ can be determined using Henry's law and phase equilibria in units of $mol.L^{-1}$. $C_{CO_2}$ is the dissolved $CO_2$ concentration in the bulk in units of $mol.L^{-1}$.

### 2.5.2 Gas-liquid equilibrium (labelled C in Figure 2-3)

In steady state the $CO_2$ remains balanced between the liquid and the gas phase according to Henry's law (Villadsen, Nielsen & Lidén, 2011: 70).

$$C^*_{CO_2}(l) = \frac{P_{CO_2}}{H_0} \quad \textbf{(2-3)}$$

$C^*_{CO_2}(l)$ is the $CO_2$ concentration dissolved in a liquid ($mol.L^{-1}$), $P_{CO_2}$ is the $CO_2$ partial pressure in a gas mixture (KPa) and $H_0$ is Henry's constant for $CO_2$ in a pure solvent ($kPa.L.mol^{-1}$). Since the fermentation medium contains various salts and organic substances, the solubility of the $CO_2$ will be affected. An empirical model such as the

one suggested by Schumpe and Deckwer (1979) should be employed to take the effect of the ions (i) and the organic substances (j) into account.

$$\log\left(\frac{H}{H_0}\right) = \left(\log\frac{\alpha_{G,0}}{\alpha_G}\right) = \sum_i (h_i + h_G)c_i + \sum_j K_{n,j}c_{n,j} \qquad \textbf{(2-4)}$$

$$= \sum_i \left(h_i + h_{G,0} + h_{G,T}(T-298.15K)\right)c_i$$

$$+ \sum_j (b_n + b_{G,0} + b_{G,T}(T-298.158K))c_{n,j}$$

Where H is Henry's constant for $CO_2$ in a medium (kPa.L.mol$^{-1}$), $c_i$ is the concentration of the ion i species (mol.L$^{-1}$) and $c_{n,j}$ is the concentration of organic substance j species (kg.m$^{-3}$).

In Equation (2-4) $CO_2$ solubility is expressed in the form of Bunsen coefficients ($\alpha_G$ and $\alpha_{G,0}$) to extend the model to a wide temperature range (Weisenberger & Schumpe, 1996).

The values of the ion-specific parameters $h_i$ (L.mol$^{-1}$) are given in Table 2-4. The other parameters used in Equation (2-4) are given in Table 2-5. $h_{G,0}$, $h_{G,T}$, $b_{G,0}$ and $b_{G,T}$ for $CO_2$ are given for temperatures between 273 and 313 K.

***Table 2-4**: Ion-specific parameter $h_i$ (L.mol$^{-1}$)*

| Ion | $h_i$ (L.mol$^{-1}$) |
|---|---|
| $Na^+$ | 0.1143 |
| $K^+$ | 0.0922 |
| $Ca^{2+}$ | 0.1762 |
| $Mg^{2+}$ | 0.1694 |
| $H^+$ | 0 |
| $Cl^-$ | 0.0318 |
| $HPO_4^{2-}$ | 0.1499 |
| $OH^-$ | 0.0839 |
| $HCO_3^-$ | 0.0967 |
| $CO_3^{2-}$ | 0.1423 |

***Table 2-5**: Parameter values of Equation (2-4)*

| Parameter | Value |
|---|---|
| $h_{G,0}$ (Weisenberger & Schumpe, 1996) | -0.0172 $L.mol^{-1}$ |
| $h_{G,T}$ (Weisenberger & Schumpe, 1996) | -0.338 x $10^{-3}$ $L.mol^{-1}$ |
| $b_n$ for yeast extract (Rischbieter *et al.,* 1996) | 7.90 x $10^{-4}$ $m^3.kg^{-1}$ |
| $b_n$ for glucose (Rischbieter *et al.,* 1996) | 6.68 x $10^{-4}$ $m^3.kg^{-1}$ |
| $b_{G,0}$ (Rischbieter *et al*., 1996) | -1.86 x $10^{-4}$ $m^3.kg^{-1}$ |
| $b_{G,T}$ (Rischbieter *et al*., 1996) | 0.010 x $10^{-4}$ $m^3.kg^{-1}K^{-1}$ |

### 2.5.3 $CO_2$-carbonate equilibrium (labelled D in Figure 2-3)

$CO_2$ and carbonate have the chemical reaction equilibrium in the steady state condition shown in Equations (2-5), (2-6) and (2-7) (Xi *et al*., 2011). These reactions occurred in the fermentation broth and also inside the cell after dissolved $CO_2$ was transported through the cell membrane. These reactions occur rapidly and equilibrium is established instantaneously. Since the dissolved $CO_2$ concentration in the fermentation broth was the independent variable under investigation, the equilibrium reactions occurring inside the cells were not considered. The reactions inside and outside the cell are expected to be similar, but the equilibrium constants may vary slightly depending on internal cell conditions.

$$CO_2 + H_2O \leftrightarrow H_2CO_3 \qquad K_1 = \frac{C^{eq}_{H_2CO_3}}{C^{eq}_{CO_2}} \qquad \textbf{(2-5)}$$

$$H_2CO_3 \leftrightarrow HCO_3^- + H^+ \qquad K_2 = \frac{C^{eq}_{HCO_3^-} C^{eq}_{H^+}}{C^{eq}_{H_2CO_3}} \qquad \textbf{(2-6)}$$

$$HCO_3^- \leftrightarrow H^+ + CO_3^{2-} \qquad K_3 = \frac{C^{eq}_{CO_3^{2-}} C^{eq}_{H^+}}{C^{eq}_{HCO_3^-}} \qquad \textbf{(2-7)}$$

Carbonic acid is very unstable in solution and is easily broken down. Equations (2-5) and (2-6) can therefore be combined as shown in Equation (2-8).

$$CO_2 + H_2O \leftrightarrow HCO_3^- + H^+ \qquad K_4 = K_1 x\, K_2 = \frac{C^{eq}_{HCO_3^-} C^{eq}_{H^+}}{C^{eq}_{CO_2}} \qquad \textbf{(2-8)}$$

$K_3$ and $K_4$ are dissociation constants with values of $K_3 = 5.3502 \times 10^{-7}$ mol.L$^{-1}$ and $K_4 = 6.1245 \times 10^{-11}$ mol. L$^{-1}$ at 39 °C (Kent & Eisenberg, 1976). $C^{eq}_{H^+}$ is the hydronium ion concentration in the solution which is derived from the pH value of the medium. $C^{eq}_{CO_2}$ in Equations (2-5) and (2-8) will be equal to $C_{CO_2}$.

### 2.5.4 Diffusion through cell membrane (labelled E in Figure 2-3)

Zou *et al.* (2011) found that there were few reports that $CO_3^{2-}$ could be used directly as a substrate by succinic acid-producing microorganisms. Although $HCO_3^-$ and $CO_2$ could be used as the co-substrate of PEP carboxylase and improve the production of succinic acid (Samuelov *et al*., 1991, referred to by Zou *et al.*, 2011), $HCO_3^-$ was much less permeable to lipid cell membranes than the uncharged $CO_2$ molecule and there was no $HCO_3^-$ transporter on the membrane of *A. succinogenes* (Badger & Price, referred to by Zou *et al.*, 2011). Gutknecht *et al.,* referred to by Lu, Eiteman and Altman *(*2009), also found that permeation of $HCO_3^-$ through the lipid membrane was insignificant. Therefore the higher concentration of $HCO_3^-$ could not promote the production of succinic acid, and carbonate and bicarbonate salts may be used as the indirect $CO_2$ molecule donor to promote succinic acid production. The $CO_2$-carbonate equilibrium that existed in the medium will re-establish inside the cell upon diffusion of these compounds into the cell.

For rod-shaped cells (Berg; Neidhardt *et al.* referred to by Lu *et al*., 2009), the $CO_2$ diffusion rate through membrane proteins is given by Equation (2-9).

$$J_{CO_2} = PA_E(C_{CO_2} - C^{eq}_{CO_{2t}}) \qquad \textbf{(2-9)}$$

The permeability coefficient P is $3.5 \times 10^{-3}$ m.s$^{-1}$ (Gutknecht *et al.* referred to by Lu *et al.*, 2009) and $A_E$ is the surface area of the cell which is assumed to be approximately the same as that of an *E. coli* cell of $6 \times 10^{-12}$ m$^2$ (Neidhardt *et al.* referred to by Lu *et al.,* 2009). $C^{eq}_{CO_{2t}}$ is the $CO_2$ concentration inside the cell. By setting Equation (2-9) equal to the maximum experimental consumption rate and calculating $C^{eq}_{CO_{2t}}$, one can determine whether this diffusion plays a significant role and whether it should be taken into account. $J_{CO_2}$ in Equation (2-9) is the flux per cell. Therefore the total amount of biomass present in the reactor and the average dry weight of an *A. succinogenes* cell needs to be quantified in order to be able to determine if this step is rate limiting.

## 2.6 Previous $CO_2$ studies of *A. succinogenes*

Most $CO_2$ studies that have been conducted to date investigate the effect of $CO_2$ partial pressure and the addition of certain carbonate and bicarbonate salts on the microorganism's metabolic activity, specifically the effect on succinic acid production. All tests to date have been performed in batch reactors. Table 2-6 provides a summary of the maximum productivity and yield obtained from the different studies and Sections 2.6.1 and 2.6.2 discuss the results.

### 2.6.1 $CO_2$ partial pressure

In these studies $CO_2$ partial pressures ranging from 0 to 140 kPa were investigated by mixing $CO_2$ and nitrogen in proportion. The $CO_2$ partial pressure influences the $C_{CO_2}$ according to Henry's law (Equation (2-3)). As can be seen from Table 2-6, there is an increase in succinic acid productivity ($P_{SA}$) with an increase in $CO_2$ partial pressure (Xi *et al.*, 2011; Gunnarson *et al.,* 2014). The maximum value of $P_{SA}$ of 1.14 g.L$^{-1}$.h$^{-1}$ was obtained at a $CO_2$ partial pressure of 100 kPa, equal to a dissolved $CO_2$ concentration ($C_{CO_2}$) of 22.7 mM (Xi *et al.*, 2011). $Y_{GLSA}$ and $Y_{AASA}$ also increased with an increase in $CO_2$ partial pressure (Van der Werf *et al.*, 1997; Xi *et al*, 2011; Gunnarson *et al.,* 2014). Maximum values for $Y_{GLSA}$ and $Y_{AASA}$ of 0.714 g.g$^{-1}$ and 4.7 g.g$^{-1}$ respectively were achieved at a $CO_2$ partial pressure of 100 kPa ($C_{CO_2}$ of 22.7 mM) (Xi *et al.*, 2011). Gunnarson *et al*. (2014) performed experiments at a $CO_2$ partial pressure of 140 kPa ($C_{CO_2}$ of 31.97 mM) and reported values for $P_{SA}$, $Y_{GLSA}$ and $Y_{AASA}$ of 0.8 g.L$^{-1}$.h$^{-1}$, 0.69 g.g$^{-1}$ and 3.46 g.g$^{-1}$ respectively. These values are lower than the maximum values obtained, possibly due to differences in feed compositions or higher starting glucose

concentrations used in Xi *et al.* (2011). Gunnarson *et al*. (2014) were able to compare their model for $C_{CO_2}$ with the actual experimental concentration by using an InPro 5000i dissolved $CO_2$ sensor (Mettler Toledo, Switzerland) and found that their model gave an accurate representation of reality.

Zou *et al*. (2011) found that when using gaseous $CO_2$ as the sole inorganic carbon provider, the $CO_2$ partial pressure had no significant effect on the succinic acid accumulation. Similarly, the concentration of the by-products acetate, formate and ethanol remained constant regardless of the $C_{CO_2}$. The authors also reported values for lactic acid at concentrations of 11.00 $g.L^{-1}$, which casts some doubt on the purity of the bacterial culture used in these experiments. McKinlay *et al*. (2007) state that lactate is not produced by *A. succinogenes* since low lactate dehydrogenase activity levels were detected in *A. succinogenes* cell extracts (Van der Werf *et al*., 1997). The only lactate dehydrogenase encoded in the *A. succinogenes* genome resembles the membrane-bound FAD-lactate dehydrogenase, which couples lactate oxidation to amino acid and sugar transport (Barnes & Kaback, 1971; Dym *et al*., 2000), and no $_{D,L}$-lactate was consumed when supplied as co-feed in a glucose fermentation (McKinlay *et al.*, unpublished data).

### 2.6.2 Supplementation of carbonate

Different carbonate salts can be added to the fermentation medium as a $CO_2$ donor. The most common salts used are $MgCO_3$, $NaHCO_3$ and $CaCO_3$. The $CO_2$ availability is strongly dependent on the dissolution rate of these salts since the carbonate/bicarbonate/$C_{CO_2}$ equilibrium is rapidly established. Under typical fermentation conditions (pH = 6.8, T = 38 ºC and atmospheric $CO_2$ pressure) the dissolved carbonate concentration is very low. As mentioned previously, *A. succinogenes* cannot use $CO_3^{2-}$ or $HCO_3^-$ as an inorganic carbon donor and therefore carbonate and bicarbonate salts added only function as indirect donors of $CO_2$. The cations $Mg^{2+}$, $Na^+$ and $Ca^{2+}$ can influence the fermentation pH and have an effect on the metabolic profile and morphology of succinic acid-producing strains (Liu *et al.,* referred to by Zou *et al.,* 2011). Zou *et al.* (2011), Xi *et al*. (2011) and Van der Werf *et al*. (1997) investigated the effect of the addition of certain carbonate and bicarbonate salts on the productivity and yield of *A. succinogenes.* The calculated $C_{CO_2}$ values of Zou *et al.* (2011) and Xi *et al.* (2011) are, however, questionable and the $CO_2$ concentrations in these studies were never measured to determine the accuracy of

the model. The maximum $C_{CO_2}$ concentration is determined by the $CO_2$ partial pressure in the gas phase. For Xi *et al*. (2011) the $CO_2$ partial pressure was equal to 0.1 MPa when carbonate and bicarbonate salts were added. Therefore the value for $C_{CO_2}$ and $C_T$ can never exceed 22.7 mM and 99.9 mM respectively. Xi *et al.* (2011) reported values for $C_T$ of up to 299.9 mM when 0.2 mol.$L^{-1}$ of $NaHCO_3$ was added. Similarly Zou *et al*. (2011) also worked at a $CO_2$ partial pressure of 101.33 kPa, which would limit the dissolved $CO_2$ concentration to 20.22 mM. Zou *et al*. (2011), however, reported values for $C_{CO_2}$ up to 159.22 mM when an amount of $MgCO_3$ higher than 11.68 g.$L^{-1}$ was added to the broth. A further stoichiometric check was done to see whether the added salt concentration was high enough to reach the saturated levels at atmospheric pressure by using Equations (2-7) and (2-8). The salt concentrations added by Xi *et al.* (2011) were high enough to reach the maximum of 22.7 mM in all the experiments. The fact that saturated conditions were maintained in all the experiments could explain why there was no significant change in productivity or yield with an increase in salt concentration. The slight increase observed when the $NaHCO_3$ concentration increased might be attributed to an increased rate of dissolution with an increase in concentration for this salt or due to the positive effect that the $Na^+$ ions have on the cell. Xi *et al*. (2011) reported the highest value for $P_{SA}$ of 1.40 g.$L^{-1}$.$h^{-1}$ when a concentration of 12.6 g.$L^{-1}$ $NaHCO_3$ was added. The highest value for $Y_{GLSA}$ of 0.757 g.$g^{-1}$ was obtained when 16.8 g.$L^{-1}$ $NaHCO_3$ was added, and the highest value for $Y_{AASA}$ of 5.2 g.$g^{-1}$ was obtained when 12.6 and 16.8 g.$L^{-1}$ $NaHCO_3$ were added (Xi *et al.,* 2011). However, the $MgCO_3$ concentrations added by Zou *et al*. (2011) could only reach the maximum $C_{CO_2}$ value of 20.22 mM when 40 g.$L^{-1}$ of $MgCO_3$ was added. This would explain why an increase in productivity and yield was observed up to a concentration of 40 g.$L^{-1}$ of $MgCO_3$, while above this concentration both productivity and yield remained constant. The highest succinic acid productivity of 0.86 g.$L^{-1}$.$h^{-1}$ was obtained when 40 g.$L^{-1}$ of $MgCO_3$ and $CO_2$ at a partial pressure of 101.325 kPa was added (Zou *et al.,* 2011). The highest yield of 0.69 g.$g^{-1}$ was obtained when 1 mol of $CO_2$ was supplied per 1 mol of glucose (Van der Werf *et al.,* 1997).

***Table 2-6**: Summary of previous work done to determine the effect of a decrease in $C_{CO_2}$ on the productivity and yield of A. succinogenes using gaseous $CO_2$ and carbonate salts as an inorganic carbon donor*

| Study | Strain | Mode of operation | Medium | Salt addition ($g.L^{-1}$) | Gaseous $CO_2$ partial pressure (kPa) | $C_{CO_2}$ (mM) | $C_X$ ($g.L^{-1}$) | $P_{SA}$ ($g.L^{-1}.h^{-1}$) | $Y_{GLSA}$ ($g.g^{-1}$) | $Y_{AASA}$ ($g.g^{-1}$) |
|---|---|---|---|---|---|---|---|---|---|---|
| Zou *et al.*, 2011 | ATCC 55618 | Batch | YE; CSL | 0 | 101.33 | 20.22 | 3.77 | 0.23 | 0.21 | - |
| | | | | 40 ($MgCO_3$) | 101.33 | 159.22 | 6.02 | 0.86 | 0.60 | - |
| | | | | 50 ($MgCO_3$) | 101.33 | 159.22 | 6.1 | 0.85 | 0.64 | - |
| | | | | 40 ($MgCO_3$) | - | 139.00 | 6.04 | 0.8 | 0.54 | - |
| Xi *et al.*, 2011 | NJ113 | Batch | YE; CSL | 0 | 100 | 22.7 | 3.05 | 1.14 | 0.714 | 4.7 |
| | | | | 20 ($CaCO_3$) | - | - | 3.02 | 1.10 | 0.716 | 4.6 |
| | | | | 16.8 ($NaHCO_3$) | - | - | 3.24 | 137 | 0.757 | 5.2 |
| | | | | 16.8 ($MgCO_3$) | - | - | 3.16 | 1.19 | 0.752 | 5.1 |
| Van der Werf *et al.*, 1997 | ATCC 55618 | Batch | YE | - | - | 100[a] | 107[b] | - | 69[c] | 0.821 |
| Gunnarsson, Alvarado-Morales, Angelidaki, 2014 | 130Z | Batch | YE | 0 | 140 | 31.97 | - | 0.8 | 0.69 | 3.455 |

[a] Mol of $CO_2$ per 100 mol of glucose

[b] Mol of cells per 100 mol glucose. Cell carbon was calculated with $CH_2O_{0.5}N_{0.21}$

[c] Mol of succinate per 100 mol of glucose

# 3 Experimental

## 3.1 Experimental setup

### 3.1.1 Microorganism

*A. succinogenes* 130Z (DSM 22257 or ATCC 55618) was acquired from the German Collection of Microorganisms and Cell Cultures (DSMZ). The culture samples were stored in a 60% $v.v^{-1}$ cryopreservation solution (glycerol) at -40 ºC. Inoculum was prepared by adding 1 mL of the cryopreservation solution, containing the microorganism, to 15 mL of sterilised Tryptone Soy Broth (TSB) and incubating for 12–24 h at 37 ºC and 150 $r.min^{-1}$.

When a significant succinic acid concentration was detected ($C_{SA} \geq 0.6$) the inoculum was added to the reactor, since this was an indication that significant growth had occurred.

### 3.1.2 Feed materials

All the chemicals were obtained from Merck KGaA (Darmstadt, Germany), unless otherwise indicated. The medium consisted of three parts that were prepared separately. The first was the growth medium which consisted of: yeast extract (16 $g.L^{-1}$), $CaCl_2.2H_2O$ (0.2 $g.L^{-1}$), $MgCl_2.6H_2O$ (0.2 $g.L^{-1}$), NaCl (1 $g.L^{-1}$), sodium acetate (1.36 $g.L^{-1}$), $Na_2S.9H_2O$ (0.16 $g.L^{-1}$) (to ensure anaerobic conditions) and Antifoam Y-30 (0.5-1 $mL.L^{-1}$.) (Sigma-Aldrich, St. Louis, USA). The second part was the phosphate buffer consisting of $KH_2PO_4$ (3.2$g.L^{-1}$) and $K_2HPO_4$ (1.6 $g.L^{-1}$). The final part was glucose prepared at a concentration of 25 $g.L^{-1}$. Glucose is a hemiacetal in equilibrium with the open chain aldehyde sugar. Aldoses readily bond to amines to make products, many of which are irreversible and cannot be broken down by bacteria (Black, 1997). Therefore the three parts were autoclaved separately at 121 ºC for 60 minutes to prevent unwanted reactions between the different components and mixed when the mixtures had cooled to room temperature. $CO_2$ (g) (Afrox, Johannesburg, South Africa) was fed into the recycle line at different vvm values ranging between 0 and 15% vvm. Vvm refers to the volumetric flow rate of gas per reactor volume in units of $min^{-1}$.

### 3.1.3 Fermentation setup

The reactor setup used is shown in Figure 3-1. The reactor consisted of a glass cylinder contained between an aluminium base and head. The reactor had an external recycle line to provide successful agitation at flow rates of 72-102 mL.min$^{-1}$. The working volume of the reactor was 357.75 mL. The pH and temperature were measured using a Ceragel CPS71D glass probe (Endress & Hauser, Gerlingen, Germany) housed within an aluminium sheath and connected in-line with the recycle line. The pH was controlled at 6.8 using a Liquiline CM442 (Endress & Hauser, Gerlingen, Germany) where an internal relay controlled the dosing of 10 M NaOH in an on-off fashion. The temperature was controlled at 37 ºC using a custom PID feedback controller communicating with a MR Hei-Standard No. 505-20000-00-2 hotplate. The temperature and pH control had a standard deviation of 0.09 ºC and 0.007 from the set point value respectively.

The reactor level was controlled by the outlet pump. To prevent foaming problems sufficient headspace was provided in the reactor. Additional antifoam (20% v.v$^{-1}$) was also added to the reactor head to prevent foaming.

During the last two fermentations the product resevoir was kept at low temperatures by placing it inside a refrigerator. This ensured that no further growth of *A.succinogenes* or other bacteria took place within the product bottle. This was done in order to be able to collect samples over +24 hour time periods at steady state and perform Dry cell weight (DCW) measurements on these samples.

All the gas inlets and outlets contained 0.2 µm PTFE membrane filters (Midisart 2000, Sartorius, Göttingen, Germany). Gas was vented from the reactor via an outlet on the reactor head and passed through a foam trap which prevented foam blockage of the filter.

$CO_2$ flow rates were controlled using a Brooks 5850S mass flow controller (Brooks Instruments, Hungary). The control of the $CO_2$ flow rate is very important in these experiments and is discussed in Section 3.2.3 below. The reactor was aerated with a sparger with a pore size of ±2 mm.

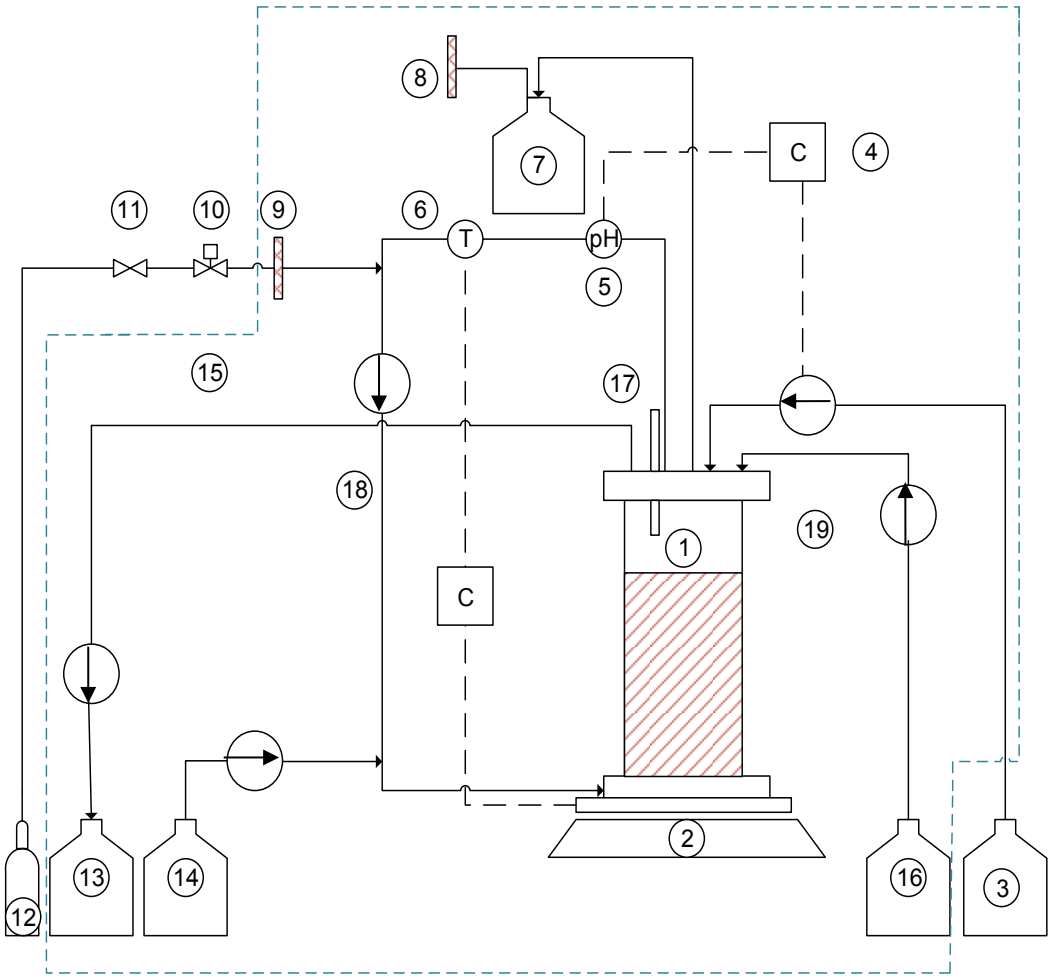


| Number | Equipment name |
|---|---|
| 1 | Reactor body |
| 2 | Hotplate |
| 3 | NaOH bottle |
| 4 | pH controller |
| 5 | pH probe |
| 6 | Temperature probe and control |
| 7 | Foam trap |
| 8 | Gas filter |
| 9 | Gas filter in $CO_2$ line |
| 10 | Gas flow controller |
| 11 | Gate valve |
| 12 | $CO_2$ cylinder |
| 13 | Product bottle |
| 14 | Feed bottle |
| 15 | Sample line |
| 16 | Antifoam bottle |
| 17 | Inoculation septum |
| 18 | Recycle line |
| 19 | Peristaltic pump |

***Figure 3-1:*** *Reactor setup used in fermentations*

### 3.1.4 Biofilm attachment

Biofilm attachment occurred on the aluminium and glass reactor internals as well as the tubing. An internal structure was added to increase the amount of biofilm attachment in the reactor. The structure selected consisted of various wooden sticks attached together with aluminium plates. These wooden sticks were covered with chopped strand mats of fibreglass. This arrangement is shown in Figure 3-2 for a smaller reactor used in exploratory runs. Data were gathered using a reactor with a larger working volume of 357.75 mL.

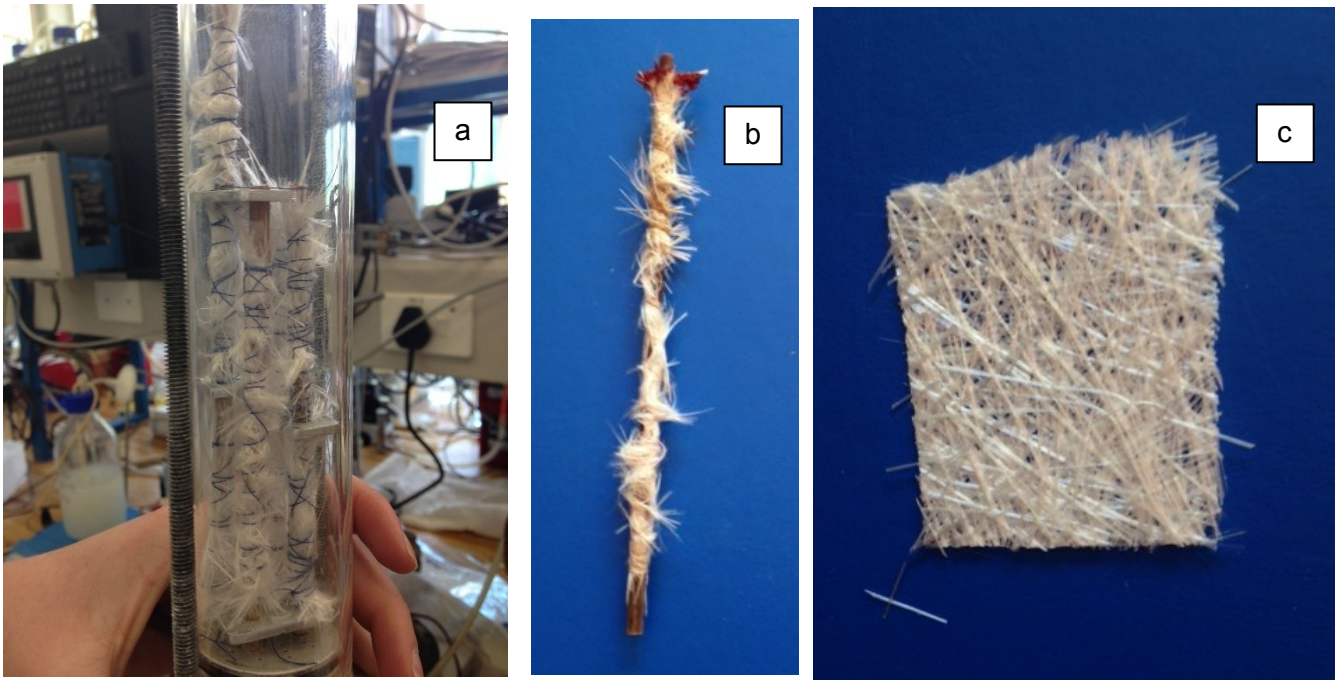


***Figure 3-2**: Images of attachment surface area. a) 3-stick arrangement in smaller reactor b) Single stick covered with fibreglass mat c) Fibreglass mat*

The arrangement using three wooden sticks caused recycle blockages and improper mixing since the biomass attached to each stick formed linkages with the biomass on the adjacent sticks until only one clump of biomass filled the entire reactor. This is shown Figure 3-3(a) and Figure 3-3(b).

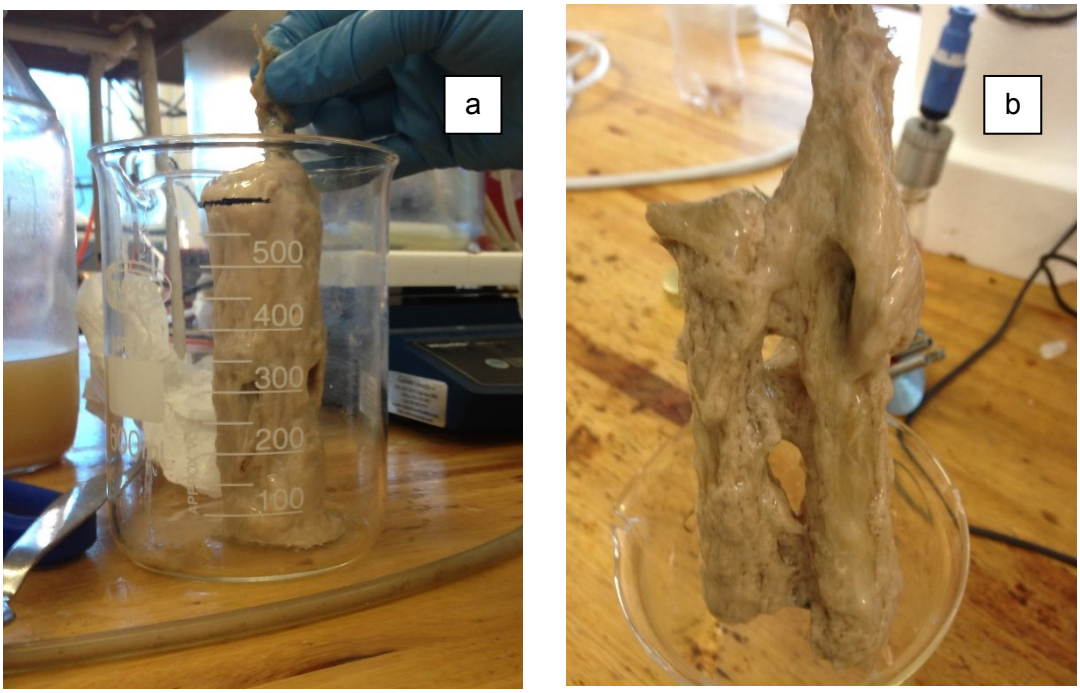


***Figure 3-3**: Attachment of biomass to covered sticks. a) Attachment structure from small reactor b) Attachment structure from big reactor*

Figure 3-4 shows what happens when proper mixing does not take place in the reactor. Gradients of colour difference can be seen in the medium. This is due to the NaOH and antifoam dosing that is not properly mixed with the rest of the medium.

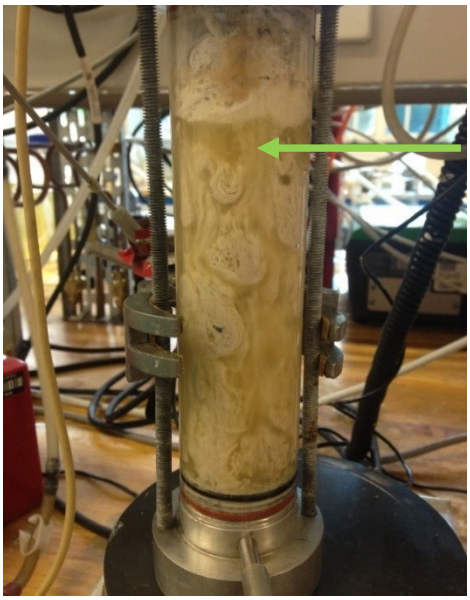

***Figure 3-4**: The green arrow shows white trails in the medium between biomass clumps indicating improper mixing conditions*

Since the problem of severe biomass accumulation in the centre of the reactor persisted even when a larger diameter reactor was used in which the sticks could be placed further apart, it was decided that a single stick would be added to the middle of the reactor to provide an attachment area for the fermentations in which experimental data were gathered.

A substantial amount of biofilm attachment occurred on the glass perimeter at the headspace of the reactor and at the liquid level in the headspace in all runs. Two possible reasons for this are that the head space provided a $CO_2$-rich environment, or that the antifoam which was dosed into the head of the reactor had a high enough viscosity to form a film at the liquid level providing extra surface area for biomass attachment. Runs where antifoam was dosed continuously into the reactor at low flow rates seemed to yield a thicker biomass layer in the headspace when compared to runs where antifoam was only added when the reactor foamed excessively.

### 3.1.5 Analytical methods

The concentrations of glucose, ethanol and the organic acids were determined using high-performance liquid chromatography. Analyses were performed using an Agilent 1260 Infinity HPLC (Agilent Technologies, USA) equipped with an RI detector and a 300 x 7.8 mm Aminex HPX-87H ion-exchange column (Bio-Rad Laboratories, USA). $H_2SO_4$ was used as a mobile phase at a flow rate of 0.6 $mL.min^{-1}$ and a column temperature of 60 ºC. Co-elution of some peaks occurred and therefore each sample was analysed with a 5 mM and 20 mM concentration of $H_2SO_4$ respectively. With increasing mobile phase acidity, the acid retention time decreases and the carbohydrate retention time remains approximately the same, leading to separation of the different peaks.

DCW measurements were performed during the last two experimental runs. Steady state samples were collected for +24 hour time periods. 80 mL of these samples were centrifuged at 4000 rpm for 20 minutes. The cells were then washed with distilled water and centrifuged at 4000 rpm for 15 minutes. After this the cell pellets were oven dried at $85^0$C for +24 hours.

## 3.2 Experimental operation

### 3.2.1 Fermentation

The fermentation was started by autoclaving the entire system (as shown by the dashed lines in Figure 3-1), excluding NaOH and the electrical components, at 121 ºC for 60 minutes. As mentioned previously, the three feed components were autoclaved separately.

After the system cooled down to room temperature, the components of the medium were mixed and sent through the reactor for 24 hours. $CO_2$ gas was allowed to flow through the reactor at a vvm between 10 and 15%. After 24 hours a sample was taken to test for possible infection. Since a fault in the antifoam feed line could also lead to infection, antifoam was dosed continuously at a low flow rate over this 24-hour time period. After 24 hours the reactor was sampled to check the lactic acid and ethanol concentrations. A high concentration of either of these would indicate that the reactor was infected. If the sample was clean, 10 mL of inoculum was aseptically injected through a silicone septum attached to the reactor head or connected to a T-piece inserted into the recycle line.

After inoculation the reactor was operated in batch conditions for approximately 12 hours to ensure that washout of the growing cells did not occur. When sufficient growth had occurred the reactor was switched to continuous mode and operated at low dilution values (0.1 $h^{-1}$) for 24–48 hours. After this time period the dilution rate was increased (to 0.3 $h^{-1}$) in order to ensure rapid growth by supplying low catabolite concentrations and thereby preventing any inhibition effects. When a succinic acid productivity of approximately 1.82 $g.L^{-1}.h^{-1}$ was reached the dilution was set to 0.124 $h^{-1}$. Initial tests showed that this is the required dilution for complete glucose conversion given a 25 $g.L^{-1}$ glucose feed.

Initial fermentations were performed to refine the procedure for the fermentations to follow and to gage at which $CO_2$ flow rate the reactor moves into a region below the $CO_2$ saturation point. The data presented in this study were gathered from three successful runs (Run 1 – Run 3) that followed after the initial fermentations. The duration of each fermentation can be found in Table 3-1. Fermentations were stopped due to infections, when the lowest operational $CO_2$ flow rate was reached or when biofilm blockages in the recycle line led to poor mixing conditions and poor pH and

temperature control in the reactor. After Run 1 the $CO_2$ mass transfer efficiency of the system was determined. The procedures for these mass transfer tests are discussed in Section 4.1. The mass transfer efficiency will be dependent on bubble size. The bubble size in turn will vary according to the pore size of the distributor. Since the same bottom distributor plate was used for all three runs it is reasonable to assume that mass transfer remained the same for different runs. The duration of the mass transfer run is also given in Table 3-1.

***Table 3-1**: Duration of fermentations*

| Fermentation | Duration (hours) | Duration (days and hours) |
|---|---|---|
| Initial Run 1 | 258 | 10 d 18 h |
| Initial Run 2 | 499.23 | 20 d 19.23 h |
| Run 1 (Run 1) | 663.17 | 27 d 15.17 h |
| Mass Transfer | 646.25 | 26 d 22.25 h |
| Run 2 (Run 2) | 720.57 | 30 d 0.567 h |
| Run 3 (Run 3) | 1 079.97 | 44 d 23.97 h |
| Total | 3 291.187 | 137 d 3.187 h |

Feed replacements were done by preparing a new feed bottle with the same composition as the first. Once again the feed components were autoclaved separately and combined after cooling to room temperature. Once combined the new feed bottle was connected to the old feed bottle. Each side of the connection was attached to a ball valve to isolate the bottles from the environment. Once these two bottles were connected the connection points and valves were placed in an oil bath at 140 ºC for 30 min to sterilise the coupling. The new feed was then transferred to the old bottle. When the transfer was complete the ball valves were closed and the new feed bottle was disconnected. A diagram of the system is shown in Figure 3-5. The dashed lines shows the parts of the system that were immersed in the oil bath.

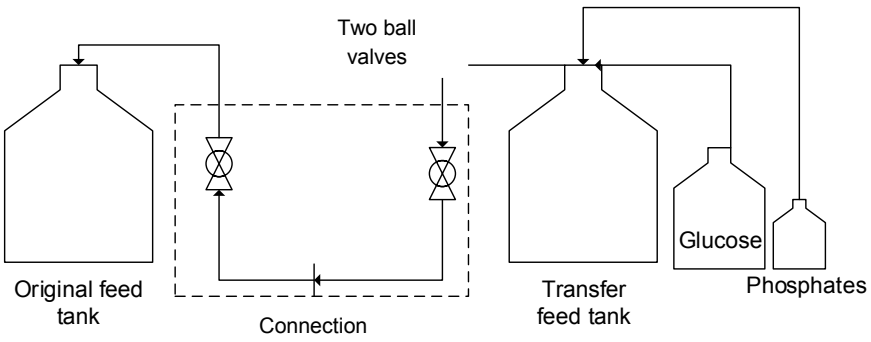


***Figure 3-5:*** *Feed transfer system*

### 3.2.2 Online monitoring

A custom Labview (National Instruments) application was used to control the reactor and record data. The instrumentation of the reactor setup was linked to the program through a c-DAQ-9184 data acquisition device (National Instruments, Hungary). The program required the following inputs: flow rates of the feed, product, antifoam and NaOH pumps, temperature setpoint and $CO_2$ gas flow rate. The following data were recorded using the program: $CO_2$ flow rate, pH, temperature, average NaOH flow rate, dilution rate and whether the NaOH pump was on/off at each time interval. The Labview interface contains the algorithm used for temperature control and is able to communicate directly with the hotplate.

### 3.2.3 Control of $CO_2$ flow rate

Optimum control of the $CO_2$ flow rate was essential in these experiments since it was the independent variable in the investigation.

To ensure optimum control, special attention was paid to the flow rate operating range of the Brooks flow meter. For the lower flow rates tested in Run 1, a Brooks meter with operating limits of 0-40 $mL.min^{-1}$ was employed. For the higher flow rates tested in Run 3, a Brooks meter with operating limits of 0-100 $mL.min^{-1}$ was employed. Table 3-2 shows the standard deviation from the set point that occurred at the highest and lowest $CO_2$ flow rates tested with the two different Brooks meters.

**Table 3-2**: Standard deviation from the set point at the highest and lowest $CO_2$ flow rate values tested

| Brooks operating limits | Highest $CO_2$ flow rate ($mL.min^{-1}$) | | Lowest $CO_2$ flow rate ($mL.min^{-1}$) | |
|---|---|---|---|---|
| | Set point | Deviation | Set point | Deviation |
| 0-40 $mL.min^{-1}$ | 21.48 | 0.01 | 0.23 | 0.006 |
| 0-100 $mL.min^{-1}$ | 10.57 | 0.02 | 0.89 | 0.02 |

From Table 3-2 it is clear that adequate control was maintained with both Brooks meters at high and low $CO_2$ flow rates.

### 3.2.4 Sampling method

When the time-averaged dosing was relatively constant, showing only a 10% fluctuation in either direction from the average, it was assumed that the system had reached a pseudo steady state. Constant values of organic acid concentrations from HPLC analysis of the product stream taken over a time period would confirm steady state.

Samples were taken from the outlet pump. The sample container was placed in an ice bath to prevent further metabolic activity from taking place during sampling. Due to the biofilm formation properties of *A. Succinogenes*, determination of dry cell weight (DCW) was difficult since unpredictable shedding events could lead to higher concentrations than would be typically observed during normal operation. This problem was addressed in Run 2 and Run 3 where steady state samples were collected over long periods of time (typically longer than 24 hours). The product bottle was stored in a fridge to terminate all metabolic activity.

### 3.2.5 Mass balance checks

Overall volume and mass balances were performed to determine the accuracy of the data obtained. Volume balances compared the volumes added from the feed, sodium hydroxide and antifoam dosing with the amount exiting to the foam trap and the product bottle over a ± 24 hour time period. Mass balances were performed by

comparing the theoretical amount of glucose consumed to produce the organic acid and ethanol concentrations to the experimentally measured glucose consumption value. A black box stoichiometric model (Villadsen *et al.*, 2011: 96-11) was used to calculate the stoichiometric amount of glucose required to produce $C_{SA}$, $C_{AA}$, $C_{FA}$, $C_{PYR}$ and $C_{ET}$. The stoichiometric amount was determined by performing elemental balances of C, H and O between the substrates and products. Glucose was the substrate, while $CO_2$ was both the substrate and the product. The elemental balances yielded three equations, and to be able to solve the system with eight unknowns, five product concentrations needed to be measured.

The experimentally measured glucose value is calculated by subtracting the exit glucose concentration from the effective inlet glucose concentration in the medium, which takes into account the diluting effect of the NaOH and antifoam dosing. The calculation for effective glucose is shown in Equation (3-1). The percentage closure is calculated as the required stoichiometric amount of glucose divided by the experimental amount of glucose consumed.

$$C_{GL,\,eff} = C_{GL,\,feed}\left(\frac{\frac{D*V}{60} - Q_D - Q_{AF}*F_{AF}}{\frac{D*V}{60}}\right) \qquad \textbf{(3-1)}$$

# 4 Results and discussion

## 4.1 $CO_2$ mass transfer and equilibrium

When investigating the influence of $CO_2$ on the productivity and yield of *A. succinogenes* the definition of the independent variable is very important. $CO_2$ flow rate or mass transfer coefficient ($k_g a_g$) could not be defined as the independent variable since these parameters will be influenced by the reactor geometry. The dissolved $CO_2$ concentration ($C_{CO_2}$) in the fermentation medium directly influences the supply of $CO_2$ to the microorganism, given the diffusion-driven rate over the cell membrane. Low supply rates will cause $C_{CO_2}$ to drop and therefore also the supply rate to the cell to decrease. Given this behaviour, $C_{CO_2}$ is therefore an effective measure of quantifying $CO_2$ availability. To quantify this independent variable, the mass transfer efficiency of the system needed to be calculated. Mass transfer experiments and repeats were conducted after the first fermentation (Run 1). A medium containing $CaCl_2.2H_2O$ (2g.L$^{-1}$), $MgCl_2.6H_2O$ (2 g.L$^{-1}$), NaCl (10 g.L$^{-1}$), sodium acetate (13.6 g.L$^{-1}$), $KH_2PO_4$ (32g.L$^{-1}$) and $K_2HPO_4$ (16 g.L$^{-1}$) was used in these experiments. The tests were performed directly after the fermentations to take into account the effect that the biomass will have on the mass transfer.

The fermentation medium was switched with the mass transfer solution after Run 1. Glucose and yeast extract are essential for the growth and maintenance of *A. succinogenes*. Since no glucose or yeast extract were added to the mass transfer solution, the biomass became metabolically inactive. Using Equation (2-4) it was seen that inclusion of glucose and yeast extract, in the calculation of the modified Henry's constant, caused the Henry's constant to increase by only 5%. The effect of these organic substances at the concentration at which they were added to the fermentation medium therefore had a negligible effect on the $CO_2$ solubility. In these tests the $CO_2$ flow rate was varied in order to quantify the mass transfer coefficient as a function of gas flow rate. All tests were performed at a high dilution of 1 h$^{-1}$. This dilution was chosen to ensure that the medium was at conditions far from the saturation point specified as $C_{CO_2} < 0.7C^*_{CO_2}$. This criterion was met at all steady states as shown in Table 4-1.

At each set gas flow rate the system was allowed to reach steady state. Similar to the fermentations, steady state was defined as the state at which the time-averaged dosing was relatively constant, showing only a 10% fluctuation from the average in either direction. This measured average dosing value was used to determine the mass transfer efficiency by performing a hydronium ion (Equation (4-2)) and inorganic carbon (Equation (4-3)) balance on the system. As discussed in Section 2.5, a number of reactions and transfer steps take place when the $CO_2$ gas enters the reactor. The mechanisms that occur and are described in Sections 2.5.1 to 2.5.3 need to be taken into account when setting up the two balances in Equations (4-2) and (4-3).

The hydronium ion balance in Equation (4-2) states that the mole of sodium hydroxide dosed ($Q_D C_{OH}$) is equal to the sum of the amount of hydronium ions produced when the equilibrium reaction in Equation (2-8) occurs (given by the term $\left[\frac{K_4}{C_{H^+}}\right] Q\, C_{CO_2}$) and the amount required to increase the feed pH from 6.4 to the setpoint of 6.8 (given by the term $Q_{feed}(C_{H^+}^{feed} - C_{H^+})$). At a pH of 6.8 no carbonate formation will be present (i.e. Equation (2-7) does not take place). The $H^+$ production term ($\left[\frac{K_4}{C_{H^+}}\right] Q\, C_{CO_2}$) was derived from the equilibrium equation of the $CO_2$ reaction with water given in Equation (2-8), rewritten as shown in Equation (4-1). From Equation (4-1) we can see that there is a fixed relationship of bicarbonate to dissolved $CO_2$. $K_4$ is the equilibrium constant in Equation (2-8). A value of $K_4 = 5.35 \times 10^{-7}$ mol.L$^{-1}$ at 39 ºC is given in the literature (Xi *et al.,* 2011). However, there is a measure of uncertainty regarding the variation of $K_4$ with temperature and feed composition and therefore mass transfer tests were conducted at conditions of $CO_2$ saturation, i.e. $C_{CO_2} = C_{CO_2}^*$, to determine $K_4$ for the conditions used in this study. $CO_2$ saturation was obtained at low dilution values (D = 0.2 h$^{-1}$) and high vvm values (vvm = 15%). During saturated conditions a decrease of the vvm will not decrease the dosing flow rate. During these conditions all the parameters in Equation (4-2) are known except the constant $\frac{K_4}{C_{H^+}}$, which can then be calculated for this specific system. From these tests the actual value of $\frac{K_4}{C_{H^+}}$ was calculated to be 4.45. Therefore $K_4$ had a value of $7.053 \times 10^{-7}$ mol.L$^{-1}$ at the conditions specified in the reactor.

$$\frac{K_4}{C_{H^+}} = \frac{C_{HCO_3^-}}{C_{CO_2}} = 4.45 \quad \textbf{(4-1)}$$

$$Q_D C_{OH} = \left[\frac{K_4}{C_{H^+}}\right] Q C_{CO_2} + Q_{feed}(C_{H^+}^{feed} - C_{H^+}) \quad \textbf{(4-2)}$$

The inorganic carbon balance simply states that the amount of $CO_2$ transferred based on the $H^+$ production from the equilibrium equations ($\left[1+\frac{K_4}{C_{H^+}}\right] Q C_{CO_2}$) is equal to the $CO_2$ mass transferred, given by $k_g a_g (C^*_{CO_2} - C_{CO_2}) V$ as discussed in Section 2.5.1. $C^*_{CO_2}$ was calculated as discussed in Section 2.5.2, taking into account the effect that the salts and organic substances will have on the $CO_2$ solubility by modifying Henry's constant.

$$\left[1+\frac{K_4}{C_{H^+}}\right] Q C_{CO_2} = k_g a_g (C^*_{CO_2} - C_{CO_2}) V \quad \textbf{(4-3)}$$

It is important to note that the balances in Equations (4-2) and (4-3) are derived for the case where the biomass is inactive. Equations (4-2) and (4-3) can be used to solve for mass transfer coefficients ($k_g a_g$) and dissolved $CO_2$ concentrations ($C_{CO_2}$) at different vvm values when the dosing flow rate ($Q_D$) and the overall flow rate (Q) are known. The calculated values are given in Table 4-1.

***Table 4-1**: Steady state mass transfer values*

| vvm (%) | $k_g a_g$ ($h^{-1}$) | $C_{CO_2}$ (mM) | D ($h^{-1}$) | $Q_D$ ($mL.h^{-1}$) | $\frac{C_{CO_2}}{C^*_{CO_2}}$ |
|---|---|---|---|---|---|
| 1.5 | 1.68 | 4.44 | 1 | 0.71 | 0.23 |
| 1 | 1.27 | 3.54 | 1 | 0.57 | 0.18 |
| 0.75 | 0.88 | 2.60 | 1 | 0.42 | 0.14 |
| 0.5 | 0.66 | 2.02 | 1 | 0.32 | 0.11 |
| 0.25 | 0.35 | 1.14 | 1 | 0.18 | 0.06 |
| 0.125 | 0.22 | 0.72 | 1 | 0.12 | 0.0386 |

The mass transfer results of the first run and repeat are graphically shown in Figure 4-1.

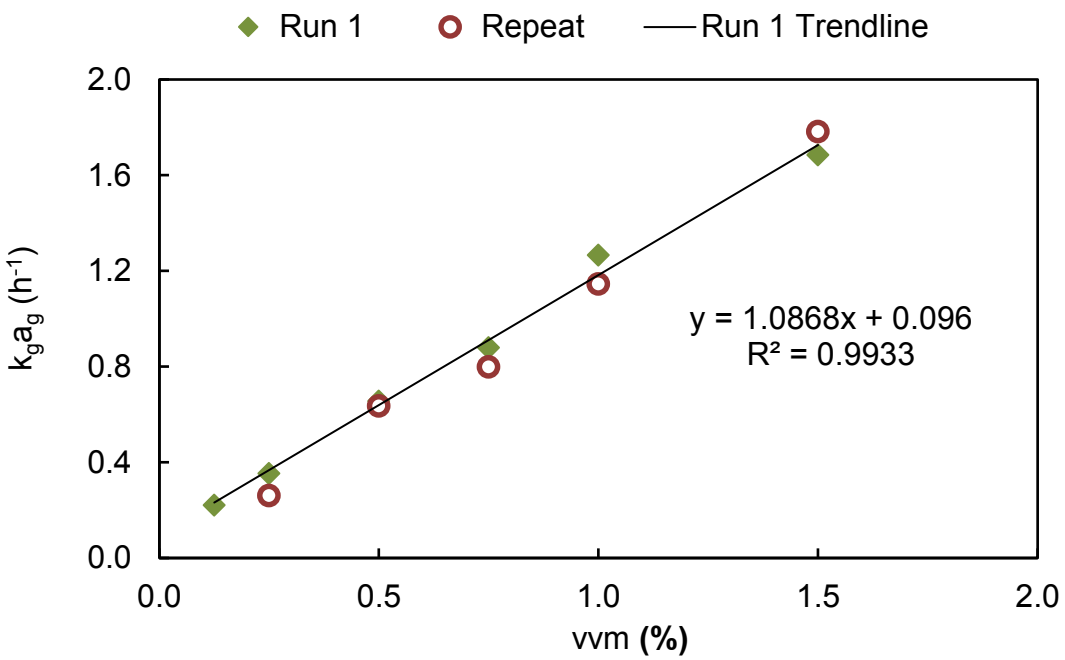


***Figure 4-1**: The gas-based mass transfer coefficient ($k_g a_g$) as a function of different $CO_2$ rates (% vvm)*

A straight line relationship exists between $k_g a_g$ and $CO_2$ vvm. This shows that an increase in $CO_2$ vvm contributes directly to improved mass transfer and thereby an increase in $C_{CO_2}$. The biomass dissolved and systematically washed out of the reactor after the fermentation medium was replaced with the mass transfer solution. However, no difference between the first test and the repeat was seen, even though the last data point was gathered 26 days after the first. This proves that the presence of biomass in this reactor setup has no influence on mass transfer efficiency and that the procedure is repeatable.

During fermentation the effect of the $CO_2$ consumption by the active biomass had to be taken into account. Equation (4-4) was therefore used to calculate the dissolved $CO_2$ concentration in Run 1–Run 3, with $k_g a_g$ calculated from the straight line relationship in Figure 4-1 (y = 1.0868x + 0.096; where x is the vvm value and y the mass transfer coefficient).

$$\left[1+\frac{K_4}{C_{H^+}}\right] QC_{CO_2} = k_g a_g\left(C^*_{CO_2} - C_{CO_2}\right)V - r_{CO_2}V \quad \textbf{(4-4)}$$

## 4.2 Dissolved $CO_2$ and productivity

### 4.2.1 Experimental strategy

At high acid titres of $C_{SA}$ > 10 g.L$^{-1}$ the cell growth is severely inhibited, but still not zero (Brink & Nicol, 2014). At the steady state operating conditions of the reactor the basic assumption is that some growth occurs at all times, but this is countered by biomass removal. On average these two rates are similar, resulting in the observed steady state. However, if substrate is present in the outlet, a secondary, long-term effect can occur whereby the biomass in the fermenter (and the biomass in the outlet) gradually increase over extended periods while pseudo steady state prevails. This effect needs to be prevented to have a stable amount of active biomass in the fermenter. This was done by operating at conditions of complete substrate conversion.

Cellular activity is the product of the amount of active cells and their specific activity. If cell activity decreases, substrate breakthrough will occur and the lower-activity cells will accordingly be able to increase. When this occurs, the substrate loading needs to be decreased (in order to maintain low substrate in the outlet). This is done by decreasing the dilution rate (D) correspondingly with the decrease in cell activity. The amount of biomass in the fermenter is therefore maintained and the decrease in dilution rate will directly relate to the decrease in activity.

An additional advantage of regulating the glucose consumption by decreasing D is that the total acid concentration remains relatively stable, whereby the inhibition effect of acids, described by Lin *et al*., (2008), remains relatively constant and the true effect of $CO_2$ limitations can be observed.

### 4.2.2 Production and consumption rates

The product concentration, yield and mass balance percentage for all the steady states of Run 1–Run 3 are given in Table 4-2 below. The dosing flow rate versus time graphs are shown in Appendix A.

***Table 4-2**: Steady state values for Run 1–Run 3*

| Run | vvm (%) | $C_{CO_2}$(mM) | $CO_2$ saturation (%) | D ($h^{-1}$) | $C_{SA}$ ($g.L^{-1}$) | $C_{AA}$ ($g.L^{-1}$) | $C_{FA}$ ($g.L^{-1}$) | $C_{EtOH}$ ($g.L^{-1}$) | $C_{PYR}$ ($g.L^{-1}$) | $C_{GLCout}$ ($g.L^{-1}$) | $\Delta C_{GLC}$ ($g.L^{-1}$) | $Y_{GLCSA}$ ($g.g^{-1}$) | $Y_{AASA}$ ($g.g^{-1}$) | $Y_{AAFA}$ ($g.g^{-1}$) | Mass balance (%) |
|---|---|---|---|---|---|---|---|---|---|---|---|---|---|---|---|
| 1 | 6 | 15.36 | 0.67 | 0.124 | 12.22 | 6.37 | 4.94 | 0.34 | 0 | 1.63 | 21.50 | 0.57 | 1.92 | 0.78 | 90.79 |
| | 1.50 | 8.47 | 0.37 | 0.124 | 11.49 | 6.42 | 5 | 0.95 | 0 | 2.08 | 21.10 | 0.54 | 1.79 | 0.778 | 95.40 |
| | 1 | 7.58 | 0.33 | 0.103 | 10.96 | 6.21 | 4.93 | 0.32 | 0 | 2.97 | 20.10 | 0.54 | 1.76 | 0.79 | 90.53 |
| | 0.75 | 5.59 | 0.24 | 0.095 | 11.27 | 6.45 | 5.1 | 0.15 | 0.32 | 1.85 | 21.22 | 0.53 | 1.75 | 0.79 | 88.16 |
| | 0.5 | 3.93 | 0.17 | 0.081 | 11.23 | 6.62 | 5.24 | 0.16 | 0.29 | 1.37 | 21.54 | 0.52 | 1.70 | 0.79 | 87.66 |
| | 0.25 | 2.07 | 0.09 | 0.069 | 9.03 | 6.07 | 5.25 | 0.86 | 0.46 | 3.17 | 18.30 | 0.49 | 1.49 | 0.87 | 97.79 |
| | 0.125 | 1.58 | 0.07 | 0.055 | 7.39 | 5.66 | 5.57 | 1.12 | 0.76 | 3.09 | 18.12 | 0.41 | 1.30 | 0.98 | 93.26 |
| | 0.0625 | 1.17 | 0.05 | 0.044 | 6.83 | 5.59 | 5.05 | 1 | 0.32 | 4.06 | 16.98 | 0.40 | 1.22 | 0.90 | 91.58 |
| 2 | 8.00 | 17.63 | 0.77 | 0.124 | 11.27 | 7.00 | 5.36 | 0 | 0 | 0.313 | 20.79 | 0.54 | 1.6 | 0.77 | 89.57 |
| | 6.00 | 17.01 | 0.75 | 0.131 | 10.94 | 6.74 | 5.27 | 0 | 0 | 0.45 | 19.65 | 0.56 | 1.62 | 0.78 | 91.71 |
| | 4.00 | 16.03 | 0.70 | 0.131 | 10.54 | 6.65 | 5.19 | 0 | 0 | 0.46 | 19.59 | 0.54 | 1.59 | 0.778 | 89.93 |
| | 8.00 | 17.48 | 0.77 | 0.129 | 12.72 | 7.65 | 5.87 | 0 | 0.24 | 0.28 | 23.09 | 0.55 | 1.66 | 0.77 | 90.55 |
| | 2.50 | 14.38 | 0.63 | 0.128 | 11.23 | 7.11 | 5.8 | 0.005 | 0.40 | 0.54 | 23.12 | 0.49 | 1.57 | 0.82 | 83.20 |
| 3 | 2.96 | 12.42 | 0.54 | 0.124 | 12.22 | 7.51 | 6.24 | 0.39 | 0.075 | 0.16 | 23.40 | 0.52 | 1.63 | 0.83 | 90.78 |
| | 2.50 | 11.66 | 0.51 | 0.124 | 11.63 | 7.15 | 6.06 | 0.40 | 0 | 0.59 | 22.98 | 0.51 | 1.63 | 0.85 | 88.18 |
| | 2.00 | 10.12 | 0.44 | 0.123 | 12.39 | 7.51 | 6.36 | 0.32 | 0 | 0.32 | 23.29 | 0.53 | 1.65 | 0.85 | 91.18 |
| | 1.51 | 8.22 | 0.36 | 0.123 | 12.29 | 7.53 | 6.36 | 0.39 | 0.16 | 0.3 | 23.31 | 0.53 | 1.63 | 0.84 | 92.02 |
| | 1.50 | 8.73 | 0.38 | 0.125 | 11.04 | 7.72 | 7.08 | 0.86 | 0.044 | 0.54 | 22.99 | 0.50 | 1.44 | 0.80 | 92.68 |

In Run 1 the $CO_2$ flow rate was incrementally decreased from a maximum vvm of 8.3%. The first significant response to the $CO_2$ decrease occurred when the vvm was decreased from 1.5% (44.81% saturated, based on the atmospheric pressure in this study of 86 kPa) to 1% (40.12% saturated). During this reduction a clear drop in dosing flow rate occurred, indicative of either a decrease in cellular activity or cells dying off. This percentage decrease in dosing was used to adjust the dilution rate in order to prevent substrate breakthrough from occurring. A further incremental decrease in vvm was initiated up to the lowest vvm value of 0.0625%. With each incremental decrease the dosing flow rate response took between 28 and 90 hours to stabilise at a new steady state value. In several cases an apparent steady state was reached, but after the dilution adjustment was made a further decrease in dosing flow rate was visible. In these cases the system was allowed to reach its new steady state, whereupon a second dilution adjustment was made. The intermediate response was, however, not of interest as important data were gathered at the steady state at which the system settled after the final dilution adjustment. At this new steady state the D adjustment had to be sufficient to keep the glucose concentration below a value of 3 $g.L^{-1}$. This approach to dilution adjustment was mostly successful except in the final incremental decrease from 0.125% (8.36% saturated) to 0.0625% (6.19 % saturated), when even after the appropriate dilution adjustment the glucose concentration in the reactor reached 4 $g.L^{-1}$. Since steady state could be maintained after a decrease in $C_{CO_2}$ (even when operating at conditions of 6.19% saturation) for extended periods greater than 48 hours, a decrease in dosing flow rate was rather due to a decrease in cellular activity since the dying of cells would have led to a continuous decrease in productivity.

The aim of Run 2 and Run 3 was to investigate the effect of $C_{CO_2}$ in the intermediate region between 6% vvm and 1.5% vvm. No significant decrease in dosing flow rate was observed for any of the decreases in Run 2 or Run 3, and therefore the dosing flow rate versus time graphs are not shown in Appendix A.

When considering the effect of $C_{CO_2}$ on the productivity of *A. succinogenes*, three rates need to be considered. These are the rate of glucose consumption ($q_{GLC}$), the rate of proton production ($P_P$) and the rate of succinic acid production ($P_{SA}$). Figure 4-2 shows the change in the first two rates, $q_{GLC}$ and $P_P$, with a change in $C_{CO_2}$.

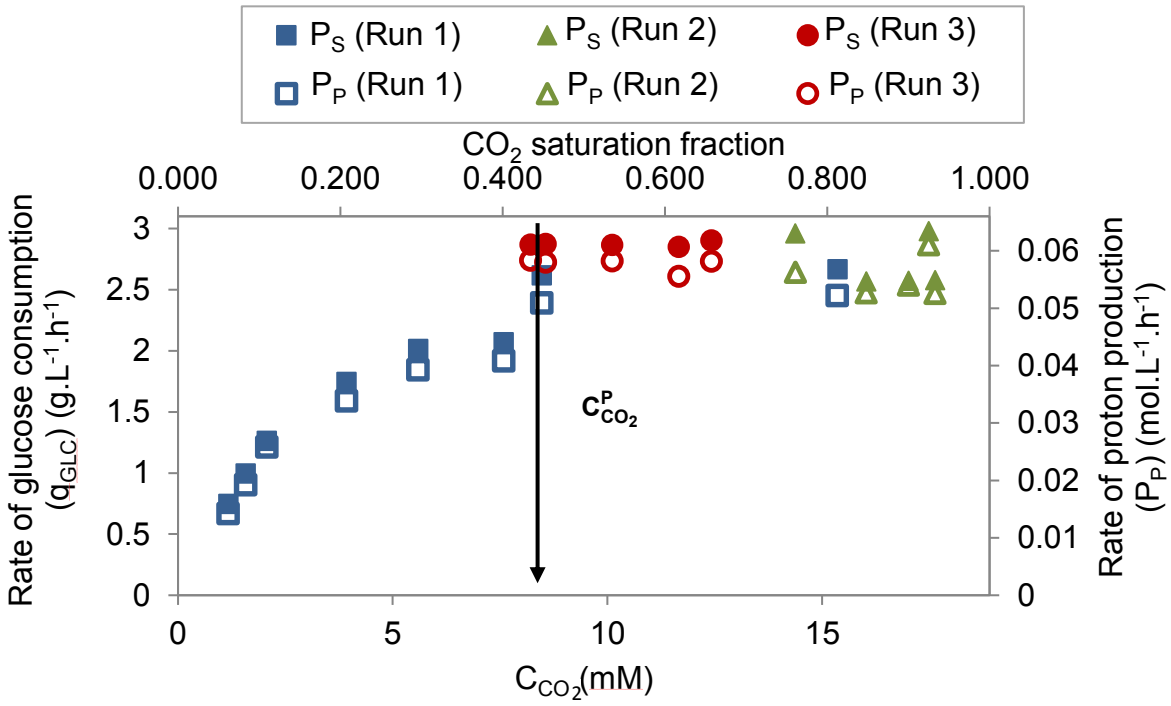


***Figure 4-2**: Decrease in glucose consumption (filled markers) and proton production rate (clear markers) with a decrease in $C_{CO_2}$ (also given in fraction $CO_2$ saturation) for Run 1 (blue), Run 2 (green) and Run 3 (red). The arrow indicates the $C_{CO_2}$ concentration at which both of these rates start to decrease ($C^P_{CO_2}$)*

From Figure 4-2 it is clear that the consumption rate of glucose as well as the proton production rate are not influenced by $C_{CO_2}$, until $C_{CO_2}$ decreases beyond a certain limiting value. Below this limiting value of $C_{CO_2}$ there is a drop in both $q_{GLC}$ and $P_P$. These rates continue to decrease as the $C_{CO_2}$ concentration decreases. This limiting threshold of $C_{CO_2}$ will be referred to as the $C_{CO_2}$ productivity threshold ($C^P_{CO_2}$). In this case $C^P_{CO_2}$ is equal to ± 8.4 mM (44.4% saturation).

Proton production rates ranged between 0.061 and 0.0141 $mol.L^{-1}.h^{-1}$, while the rate of glucose consumption varied between 2.98 and 0.75 $g.L^{-1}.h^{-1}$. From Figure 4-2 it should be noted that the rate of glucose consumption and the rate of proton production was consistently higher for Run 3 when compared to Run 1 and Run 2. This is likely due to the lower substrate concentration in the outlet ($C_{Sout}$) at similar dilution rates when compared to Run 1. Run 2 also had lower concentrations for $C_{Sout}$, but this was compensated for by the slightly higher dilution rate in Run 2, and therefore the rates for Run 1 and Run 2 were mostly similar.

The succinic acid production rate ($P_{SA}$) is shown in Figure 4-3. The same trend observed for $q_{GLC}$ and $P_P$ is observed with $P_{SA}$. Above $C^P_{CO_2}$, $P_{SA}$ is not influenced by $C_{CO_2}$. However, when $C_{CO_2}$ decreases below $C^P_{CO_2}$ $P_{SA}$ starts to decrease. Succinic acid productivities ranged between 1.64 and 0.30 $g.L^{-1}.h^{-1}$. The extent of the decrease in $P_{SA}$ is greater than for $P_P$. $P_{SA}$ decreased by 5 times while $P_P$ only decreased by 3.5 times, indicating that the production of succinic acid in *A. succinogenes* starts to decrease below $C^P_{CO_2}$, while the production rates of the other acids (contributing to $P_P$), such as acetic and formic acid, stay relatively constant or decrease to a lesser extent.

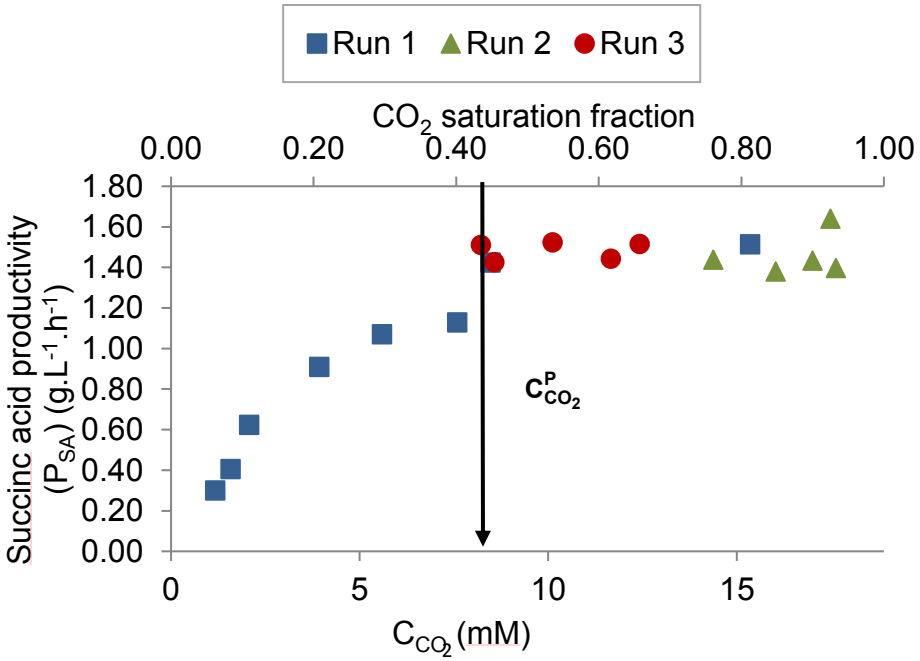


***Figure 4-3:*** *Decrease in succinic production rate ($P_{SA}$) with $C_{CO_2}$ (also given as $CO_2$ saturation fraction) for Run 1 (squares), Run 2 (triangles) and Run 3 (circles). The arrow indicates the $C_{CO_2}$ concentration at which succinic acid production starts to decrease ($C^P_{CO_2}$)*

In agreement with the observation that $P_{SA}$ is not influenced by $C_{CO_2}$ above concentrations of 8.4 mM, Zou *et al*. (2011) found that $P_{SA}$ was not affected by a change of $CO_2$ partial pressure and therefore remained constant at dissolved $C_{CO_2}$ of 20.22, 15.16 and 10.11 mM. Only a slight decrease was observed at the lowest $C_{CO_2}$ (5.05 mM) tested. However, Xi *et al*. (2011) and Gunnarson *et al.* (2014) showed that the final succinic acid titre and productivity were enhanced when increasing the $CO_2$

partial pressure from 0 to 100 kPa ($C_{CO_2}$ of 0, 5.67, 11.3, 17, 22.7 mM) and 101.325 to 140 kPa ($C_{CO_2}$ of 23.16 and 31.97 mM) respectively. Zou *et al*. (2011), Xi *et al.* (2011) and Gunnarson *et al.* (2014) all performed batch fermentations and only the final cumulative outcome was reported. However, formation of succinic acid varies appreciably during a batch run as there is an initial growth period and a product inhibition stage at a later stage in the fermentation (Corona-González *et al*., 2008; Lin, *et al.*, 2008). Variations in succinic acid production will cause a variation in $CO_2$ consumption and therefore a change in $C_{CO_2}$. $C_{CO_2}$ can be estimated from $CO_2$ partial pressure at saturation, although the broth might not be saturated since the gas-liquid mass transfer might be limiting. It is therefore more effective to use a continuous system, in which $C_{CO_2}$ can be kept constant, to see the true effect of $C_{CO_2}$ on yield and productivity.

## 4.3 Distribution

### 4.3.1 Product concentrations and flux analysis

A similar trend to productivity was observed with product distribution. Figure 4-4(a) gives the concentration of succinate ($C_{SA}$), acetate ($C_{AA}$) and formate ($C_{FA}$) in the outlet with a change in $C_{CO_2}$. Figure 4-4(b) shows how the ethanol ($C_{ETH}$) and pyruvate ($C_{PYR}$) concentrations in the outlet changed with respect to $C_{CO_2}$.

On average the mass balances (values given in Table 4-2) closed to 91% with a standard deviation of 3.04%. This shows that more glucose is consumed than is required for the metabolite production. This is in agreement with previous continuous fermentations with *A. succinogenes* biofilms where incomplete mass balance closures were observed on glucose (Bradfield & Nicol, 2014), xylose (Bradfield & Nicol, 2016; Bradfield *et al.,* 2015) and corn stover hydrolysate (Bradfield *et al.,* 2015). Taking the DCW measurements into account, the mass balance on average closed to 102% with a standard deviation of 6.41%. This shows that the extra glucose might have been used for the production of new cells that will replace the older cells that systematically washes out of the system.

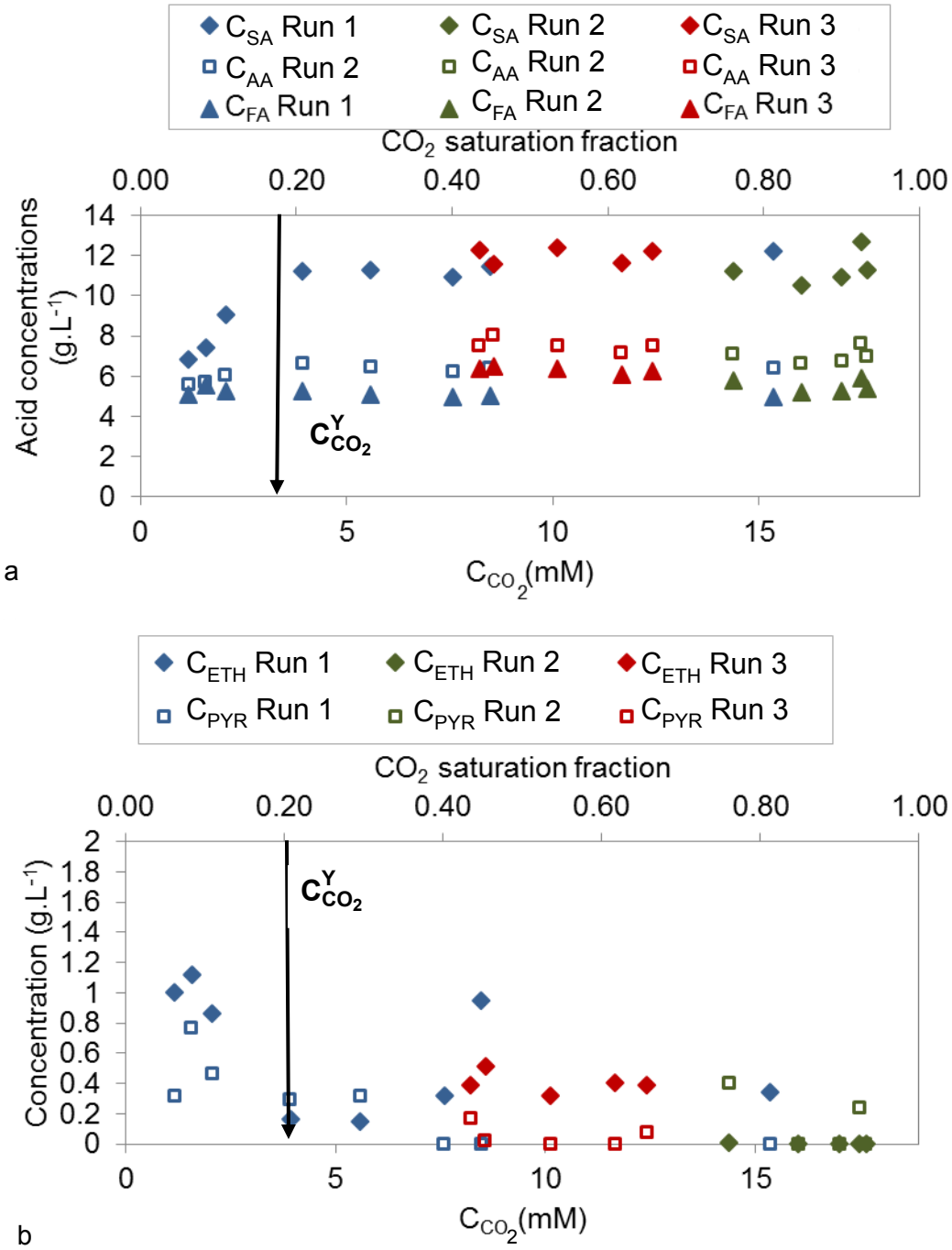


***Figure 4-4**: Product concentration in outlet with a change in $C_{CO_2}$ 5(a) $C_{SA}$, $C_{AA}$ and $C_{FA}$ versus $C_{CO_2}$, 5(b) $C_{ETH}$ and $C_{PYR}$ versus $C_{CO_2}$. The arrow indicates the $C_{CO_2}$ concentration at which a shift in product distribution starts to occur ($C^{Y}_{CO_2}$)*

From Figure 4-4(a) it can be seen that above a specific $C_{CO_2}$, in this case ± 4 mM, $C_{SA}$ stays constant at an average value of 11.6 $g.L^{-1}$ with a standard deviation of 0.63 $g.L^{-1}$. Below 4 mM $C_{SA}$ decreases to the lowest value of 6.83 $g.L^{-1}$ obtained at the lowest $C_{CO_2}$ investigated. $C_{AA}$ was also constant above a $C_{CO_2}$ of 4 mM, but showed

a slight decrease (to 88% of the original value) when $C_{CO_2}$ dropped below 4 mM. $C_{FA}$ remained fairly stable at a value of 5.135 $g.L^{-1}$ with a standard deviation of 0.2 $g.L^{-1}$ across the whole range of $C_{CO_2}$ values investigated. Zou *et al*. (2011) also observed an increase in $C_{AA}$ while $C_{FA}$ remained constant with an increase in dissolved $CO_2$ concentration, and attributed this to the fact that higher $CO_2$ levels led to an increase in PEP carboxykinase activity, which in turn competitively inhibited certain key enzymes among which was pyruvate formate-lyase. Both $C_{AA}$ and $C_{FA}$ was higher in Run 3 when compared to the values obtained for Run 1 and Run 2. This can be attributed to a change in pH that occurred towards the end of Run 3 as the pH probe started to drift. The pH of the product was measured at the end of Run 3 and found to be 7.2. As mentioned in Section 2.3, Xi *et al*. (2011) tested the effect of pH on enzyme activity. Their analysis showed that PYK (pyruvic acid kinase) activity increased with increasing pH, while PCK (phosphoenolpyruvate carboxykinase) activity did not. The maximum PYK activity occurred at pH 7.4, which was 1.65 times higher than at pH 6.8. PCK activity at pH 7.4 was 0.66 times of the value obtained at pH 6.8. The highest $Y_{AASA}$ and $CO_2$ fixation values were therefore obtained at pH 6.8. This phenomenon could explain the elevated $C_{AA}$ and $C_{FA.}$ However, the values of $C_{SA}$ remained more or less the same as in Run 1 and therefore the PCK activity does not seem to be influenced by the increased pH. The higher pH, leading to elevated values for $C_{AA}$ and $C_{FA,}$ could also explain the increased $q_{GLC}$ and $P_P$ values observed in Run 3, in comparison to Run 1 and 2.

Figure 4-4(b) shows that the $C_{ETH}$ is typically very low, with an average of 0.26 $g.L^{-1}$. However, below a certain $CO_2$ concentration there is a clear increase in $C_{ETH}$ up to a value of 1 $g.L^{-1}$, which was observed at the lowest $C_{CO_2}$value investigated. This increase in ethanol at low values of $C_{CO_2}$ is in agreement with Van der Werf *et al.* (1997). Zou *et al.* (2011) suggest that this is due to the higher activity of PEP carboxykinase (at higher values of $C_{CO_2}$), which competitively inhibits the ethanol dehydrogenase. However, as discussed later in this section, $C_{ETH}$ is rather thought to be produced with the aim to keep the redox of the system balanced. The pyruvate concentration increased slightly with a decrease in $C_{CO_2}$ below a value of 7.58 mM, but remained below 0.76 $g.L^{-1}$.

The point at which $C_{SA}$ and $C_{AA}$ decrease and where $C_{ETH}$ starts to increase occurs at exactly the same $CO_2$ value, in this case found to be in the vicinity of 4 mM (21.16% saturated). At this concentration a clear shift in the product distribution occurred. The $C_{CO_2}$ value at which this occurs will now be referred to as the $CO_2$ threshold at which metabolite distribution is affected ($C^{Y}_{CO_2}$).

In order to interpret what is happening with the concentrations in the outlet we need to consider the metabolic flux network of *A. succinogenes* shown in Figure 2-2. Special consideration should be given to the active pathways in the C3 leg of the network. One way to determine which of these pathways are active is to compare the molar ratio of $C_{FA}$ to $C_{AA}$. If this ratio is found to be equimolar, i.e. the carbon flux in the C3-pathway was equally split between the formation of $C_{AA}$ and $C_{FA}$, it is proof that all the carbon flux in the C3-pathway passed through the pyruvate formate-lyase route and that none of the formate formed was converted to $CO_2$ and NADH. This would mean that no dehydrogenase enzymes were active in the system. However, since ethanol is formed at lower values of $C_{CO_2}$ and therefore the mole of acetyl-CoA is now not only used for the production of acetate but also ethanol, it is necessary to compare the amount of acetyl-CoA (i.e. the sum of acetate and ethanol) with the amount of formate formed in order to test for the presence of dehydrogenase. This comparison is shown in Figure 4-5.

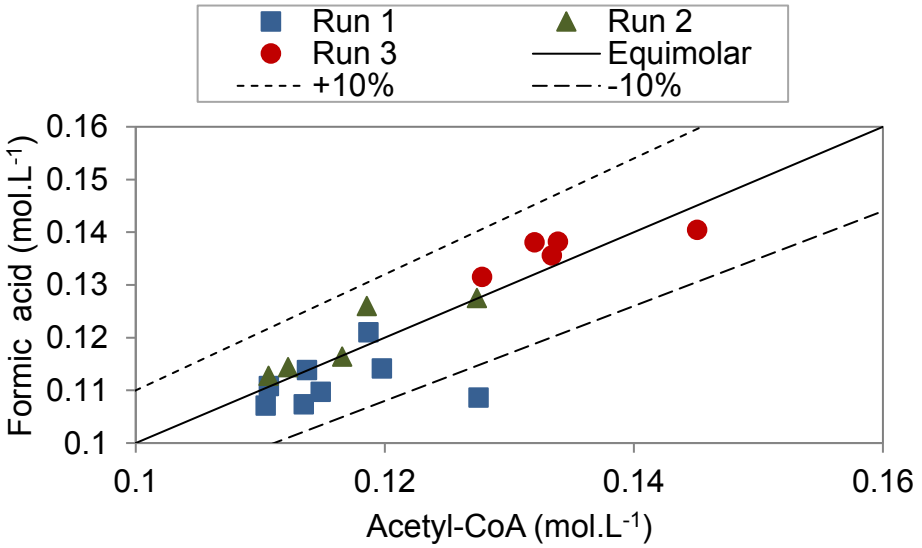


***Figure 4-5:*** *Parity plot of formic acid and acetyl-CoA. The equimolar line (solid) represents the scenario when no dehydrogenase enzymes are present*

From Figure 4-5 it can be seen that the ratio stays well within the 10% range of the equimolar line even at a low $C_{CO_2}$. From this we can conclude that no dehydrogenase enzymes are present and that pyruvate is therefore solely converted in the pyruvate formate-lyase route.

Since succinic acid is the product of interest in these studies, the fraction of the total glucose flux that enters the C4-pathway is of great importance. From the mass balances it is clear that there is a discrepancy between the glucose consumption based on HPLC analysis and the glucose consumption that can be accounted for by looking at the product formation. When calculating the fraction of glucose flux to the C4-pathway, the glucose consumption based on product formation should be used. The C4-pathway flux was taken as the flux value just after the PEP split before the incorporation of inorganic carbon in the form of $CO_2$.

Figure 4-6 shows how the C4-pathway flux fraction ($f_4$) changes with the $C_{CO_2}$.

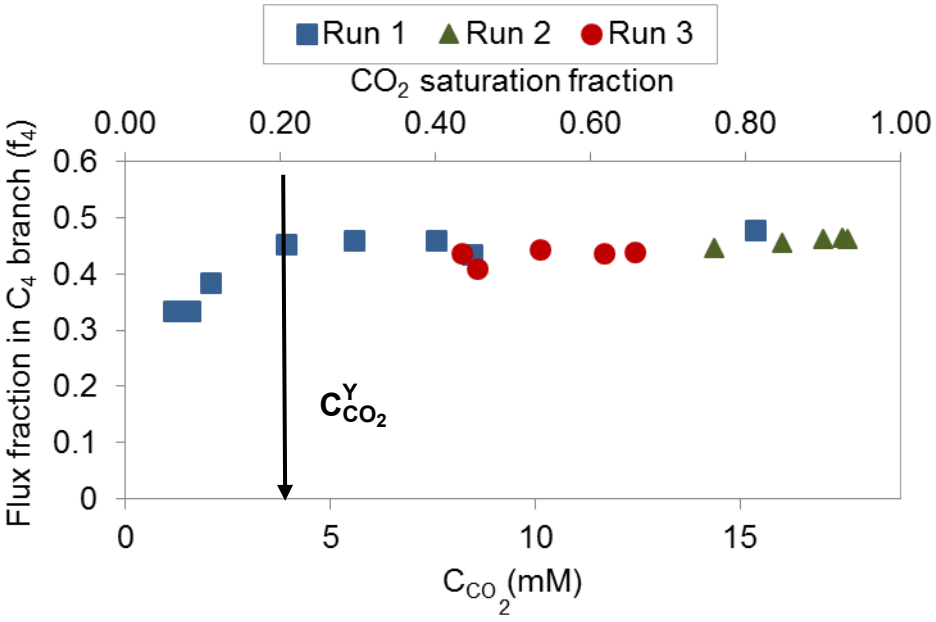


***Figure 4-6**: Fraction of total glucose flux directed towards the C4-pathway. The arrow indicates the $C_{CO_2}$ concentration at which a shift in product distribution starts to occur ($C^{Y}_{CO_2}$)*

In Figure 4-6 we see the same pattern as in Figure 4-2 and Figure 4-3. Once again it is clear that a shift in the metabolite distribution occurs at $C_{CO_2}^{Y}$. The reason for this flux shift is discussed in Section 4.4.

### 4.3.2 Redox balances

Redox balances were performed by considering the NADH contributions from the overall balanced metabolic network pathways present in *A. succinogenes* shown in Figure 2-2, with no dehydrogenase enzymes active. The pathways can be either oxidative or reductive, where a net production is viewed as oxidative and a net consumption is viewed as reductive. In a redox-balanced system the net NADH of the oxidative and reductive pathways should be zero.

Equation (4-5) shows the overall balanced equation for the production of acetic acid, and Equation (4-6) shows the balanced equation for pyruvic production. These are the only oxidative reactions in the metabolic network.

$$GL \rightarrow 2NADH+2FA+2AA \quad \textbf{(4-5)}$$

$$GL \rightarrow 2PYR + 2NADH \quad \textbf{(4-6)}$$

Equations (4-7) and (4-8) give the overall balanced equations for the production of succinic acid and ethanol respectively. They are the reductive parts of the metabolic network.

$$GL + 2CO_2 + 2NADH \rightarrow 2SA \quad \textbf{(4-7)}$$

$$GL + 2NADH \rightarrow 2FA + 2ETH \quad \textbf{(4-8)}$$

Figure 4-7 compares the amounts of NADH produced (when producing acetate and pyruvate) to the amount consumed (to produce succinate and ethanol) for Run 1 at each $CO_2$ saturation fraction.

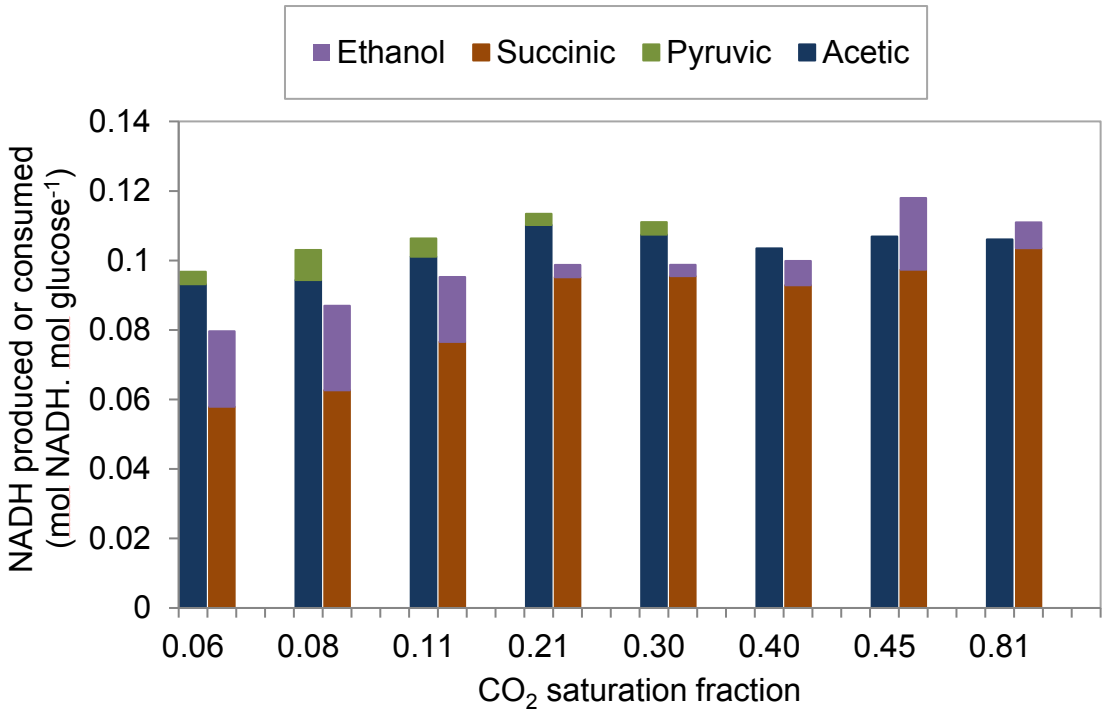


***Figure 4-7**: Amount of NADH consumed when producing succinate (brown) and ethanol (purple) versus amount of NADH produced when producing acetate (blue) and pyruvate (green) when the $CO_2$ saturation fraction is varied*

From Figure 4-7 it is evident that in all cases, except at the two highest $CO_2$ concentrations tested, more NADH was produced (blue and green stacked bars) than consumed (purple and brown stacked bars). These results are in contrast to what has been observed in previous experiments in which more NADH was consumed than produced (Bradfield & Nicol, 2014). Bradfield and Nicol (2014) hypothesised that the excess NADH might be obtained from an active pentose phosphate pathway (PPP). NADPH is produced in the PPP pathway, which can then be converted to NADH by transhydrogenase. Comparison of the results of Bradfield and Nicol (2014) and the results of this study is, however, difficult since their fermentation medium contained corn steep liquor, which might cause the metabolism of *A. succinogenes* to behave differently to when only yeast extract is used. To date no studies have been performed to test whether the PPP is active when only a yeast extract medium is used. Lu *et al.* (2009) found that the flux into the PPP increased from 0.04 at 3% $CO_2$ to 0.17 at 50%

$CO_2$ for *E. coli* AFP111 in a defined medium. If the PPP is active in a fermentation with *A. succinogenes* in a yeast extract medium and the flux to the PPP behaves similarly to that of *E. coli* with a change in $C_{CO_2}$, this might explain why there is an overconsumption of NADH at high values of $C_{CO_2}$, while no overproduction of NADH occurs at low values of $C_{CO_2}$ when the PPP flux is low.

If the PPP is not active another possible explanation for the overproduction of NADH is the failure to detect a missing metabolite. However, it is suspected that in this study it is more likely to be due to inaccuracy of the ethanol measurements. The low ethanol concentrations were difficult to detect using the HPLC method. Evaporation of ethanol also occurred, which could explain why the actual values were lower than the theoretically required ethanol concentrations that would satisfy the redox balance. The difference in NADH produced versus NADH consumed becomes more evident with decreasing $C_{CO_2}$ values, where the ethanol concentration starts to play a more significant role. The values for $C_{ETH}$ that would satisfy the redox balance was calculated and are shown in Figure 4-8 against the $CO_2$ saturation fraction.

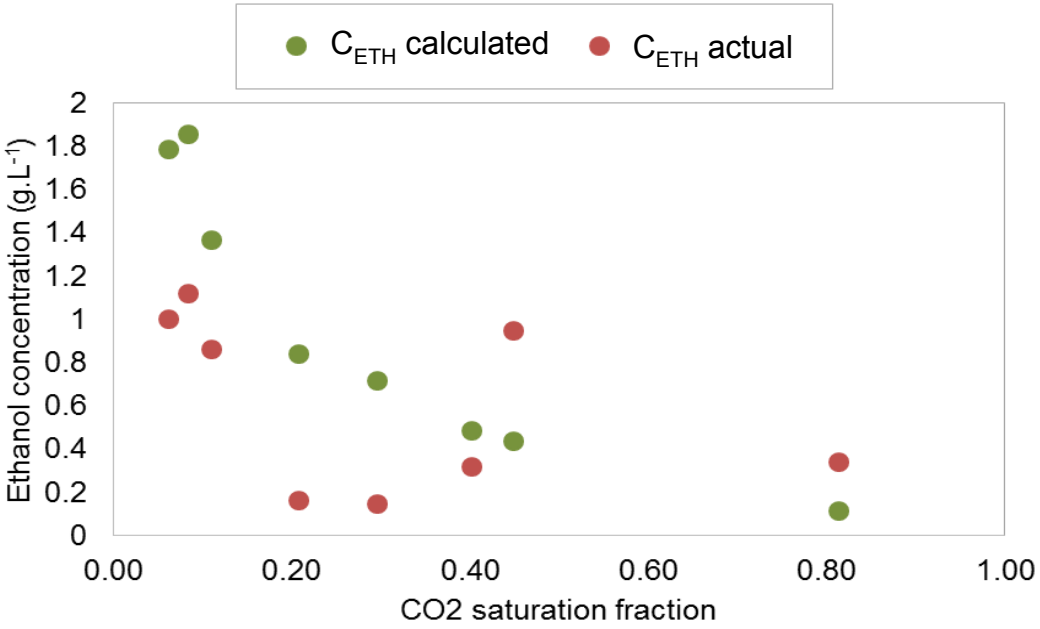


***Figure 4-8**: $C_{ETH}$ required to satisfy the redox balance*

Figure 4-8 shows the expected trend of an increase in $C_{ETH}$ as the $CO_2$ saturation fraction decreases. An error in the $C_{ETH}$ measurements is therefore a likely explanation for the redox imbalance.

## 4.4 Effects of low-dissolved $CO_2$ concentrations

The productivity and yield stay constant with a decrease in $C_{CO_2}$ up to 8.4 mM ($C^{P}_{CO_2}$). At this point the $CO_2$ consumption starts to decrease. This leads to decreased PEP carboxykinase reaction activity and a reduction in the production of succinic acid. The glucose consumption rate also decreases, while the product distribution remains constant. In this region the ATP generation of the cells will start to decrease and therefore less energy will be available for maintenance processes. However, the organism will still remain viable as can be seen by the prolonged steady state operation achieved at these conditions. As $C_{CO_2}$ decreases further and drops below a concentration of 4 mM ($C^{Y}_{CO_2}$), the succinic acid productivity continues to decrease, although a shift in the metabolite production also starts to occur. This metabolite shift occurs at the PEP node which serves as branch point between the C3- and C4-pathway. The rate limitations at the PEP node necessitates that flux be directed to the C3-pathway. The organism starts producing more ethanol as the total carbon flux towards the C4-branch starts to decrease. The flux shift to the C3-pathway makes sense when the redox balance is considered. Ethanol formation consumes two NADH molecules and can therefore serves as a redox sink in the central metabolism as an alternative to the C4-pathway. The different regimes are illustrated in Figure 4-9. The question, however, remains whether there is any benefit for ATP production with an increase in the C3-flux. Figure 4-10 shows the theoretical calculated molar yield of ATP on glucose ($Y_{SATP}$) and the molar yield of ethanol on glucose ($Y_{SE}$) with a decrease in the fraction of the total carbon directed to the C4-pathway. These calculations were based on the metabolic network shown in Figure 2-2, with the redox balance specified to have no dehydrogenase activity (only pyruvate formate-lyase active). $Y_{SATP}$ decreases as the flux towards the C3-pathway increases (the C4-pathway flux decreases). No ATP advantage is obtained with a shift in the carbon flux to the C3-pathway. Therefore this shift is solely regulated by the primary need of the organism to balance the redox where the glucose uptake does not decrease in proportion to the succinic acid flux. Therefore there is a further decrease in ATP production at low conditions of $C_{CO_2}$. However, the organism still seems to be viable at these conditions as can be seen by the extended steady state that could be maintained at the low-dissolved $CO_2$ concentrations.

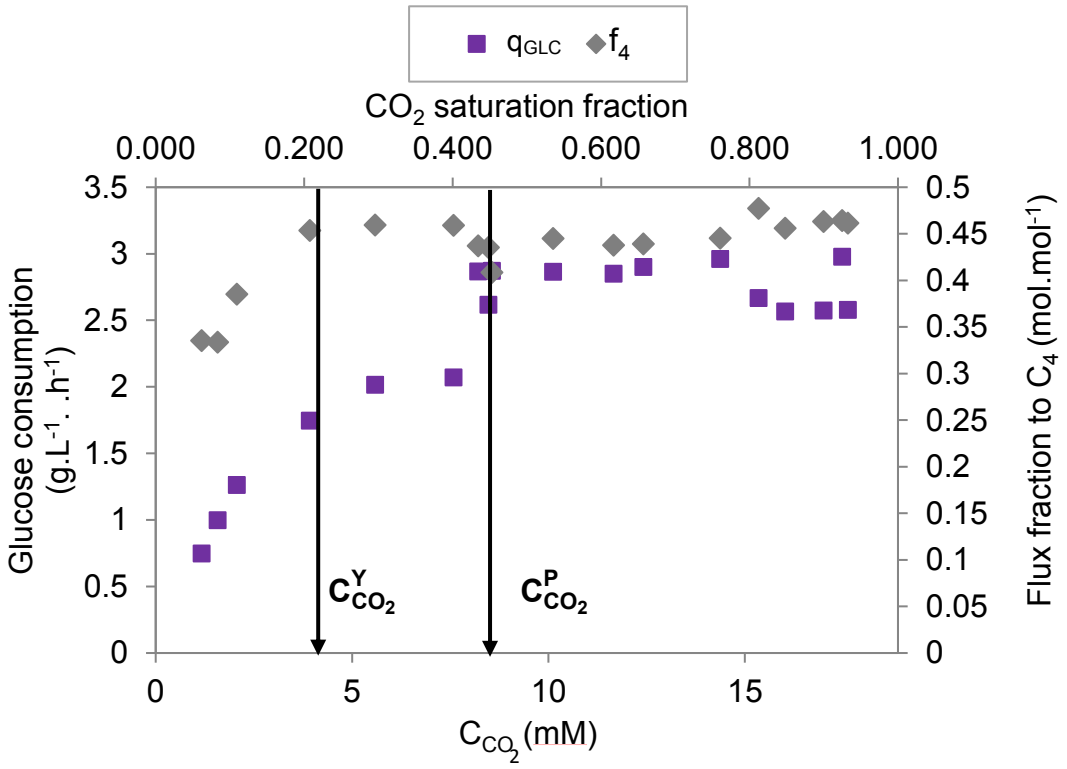


***Figure 4-9**: Concentration of $CO_2$ where change in productivity and distribution takes place*

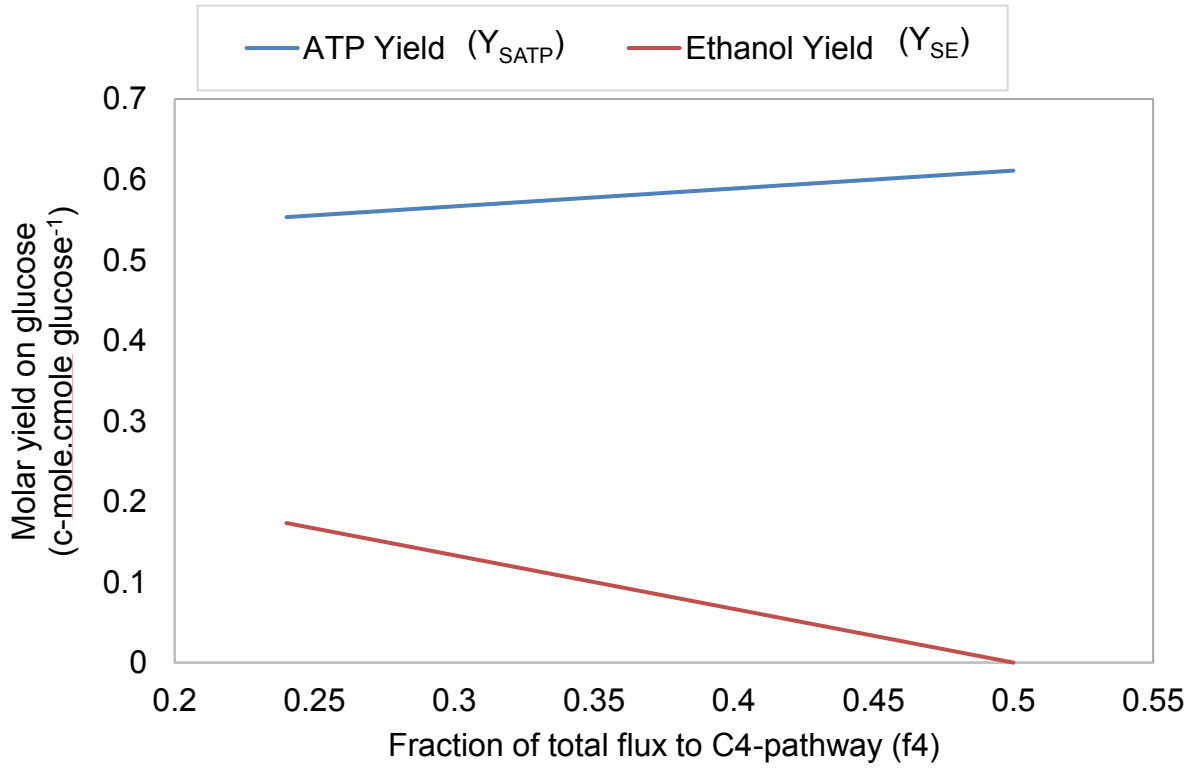


***Figure 4-10:** Change in molar yield of ATP on glucose ($Y_{SATP}$) and molar yield of ethanol on glucose ($Y_{SE}$) as the fraction of total flux into the C4-pathway ($f_4$) decreases*

## 4.5 Rate limiting factors

When considering how $CO_2$ limits succinate production the following mechanisms should be taken into consideration: 1) the $CO_2$ gas-to-liquid mass transfer, 2) the $CO_2$ carbonate equilibrium in the broth, 3) diffusion of $CO_2$ across the cell membrane, 4) the $CO_2$-carbonate equilibrium inside the cell, and 5) the availability of PEP carboxykinase and enzyme kinetics.

Lu *et al.* (2009) did an experiment using modified *E. Coli* to determine exactly which of these mechanisms could be limiting. Their model predicted that enzymatic processes are rate limiting over most of the range of gas phase $CO_2$ concentrations, but the reason for the limitation may change. At very high $CO_2$ concentrations, the activity of the enzyme likely limits $CO_2$ utilisation. At intermediate $CO_2$ concentrations (10–30% $CO_2$ in gas phase at 1 atm), the intracellular conversion of dissolved $CO_2$ into bicarbonate could limit utilisation. Only at very low $CO_2$ concentrations (2-3%) would mass transfer limit $CO_2$ utilisation. It is interesting to note that the transfer of $CO_2$ across the cell membrane was not found to be limiting.

The rate limiting mechanism in this study was most likely either the enzyme kinetics or the internal $CO_2$ concentration. When the internal $CO_2$ concentration is limiting it can either be due to slow transfer of $CO_2$ across the cell membrane or due to limitations in the external gas-liquid mass transfer. In order to determine which mechanism is limiting the amount of total biomass inside the reactor needs to be quantified in order to see whether the transfer across the membrane could be limiting by using Equation (2-9). Once the transfer of $CO_2$ across the membrane is quantified the intracellular $CO_2$ concentration can be determined in order to establish whether enzyme kinetics or internal $CO_2$ concentration is limiting. If the internal $CO_2$ concentration is limiting it should be determined if this is due the external availability of $CO_2$ or the transport of $CO_2$ across the membrane.

It is important to determine the mechanism that limits $CO_2$ utilisation to see where improvement can be made. For example, Lu *et al*. (2009) suggest that at intermediate $CO_2$ concentrations, where availability of intracellular bicarbonate is limiting, the carbonic anhydrase enzyme which catalyses the hydration of $CO_2$ to $HCO_3^-$ can be overexpressed.

# 5 Conclusions

The dissolved $CO_2$ concentration ($C_{CO_2}$) in the fermentation broth plays an important role in the production of succinic acid by *A. succinogenes*. Three distinct regimes can be defined in which the organisms behave differently based on $C_{CO_2}$. When $C_{CO_2}$ is higher than 8.4 mM (44.4% saturation at an atmospheric pressure of 86 kPa), the succinic acid productivity and the yield stays constant. In this regime the $CO_2$ consumption is not limited and the organism therefore functions optimally. Below a $C_{CO_2}$ value of 8.4 mM a drop in productivity is seen. This $CO_2$ threshold was labelled the $C_{CO_2}$ productivity threshold ($C^P_{CO_2}$). In the regime $C_{CO_2} \leq C^P_{CO_2}$ there was a decrease in the rate of proton production ($P_P$), the rate of glucose consumption ($q_{GLC}$) and the rate of succinic acid production ($P_{SA}$). These three rates decreased to 28.01, 27.26 and 19.87% of the original value, respectively at the lowest $C_{CO_2}$ value investigated.

A further reduction in $C_{CO_2}$ shows that the yield stays constant while the productivity decreases. Below 4 mM (21.16 % saturation at an atmospheric pressure of 86 kPa), however, the productivity continues to decrease together with a shift in total carbon flux away from the C4-pathway (succinic acid producing pathway) towards the C3-pathway (by-product producing pathway). The $C_{CO_2}$ value at which this metabolite shift occurs was defined as $C^Y_{CO_2}$. The fraction of total glucose flux directed towards the C4-pathway decreased from 0.48 to 0.33 at the lowest $C_{CO_2}$ value investigated. Below $C^Y_{CO_2}$ there was a slight decrease in the acetic acid by-product to 88% of the initial value, while the formic acid concentration remained stable. Above a $C_{CO_2}$ value of 4 mM the ethanol concentration was low and stable at an average value of 0.26 $g.L^{-1}$, an increase in the ethanol by-product concentration was visible at $C_{CO_2} \leq C^Y_{CO_2}$. Ethanol production consumes two NADH molecules in *A. succinogenes* and therefore serves as a redox sink when the succinate production decreases. The flux shift to the C3-pathway has no added benefits for ATP production. However, it was seen that the organism is still viable even at the lowest $C_{CO_2}$ values investigated and seems to have enough energy for maintenance at these low $CO_2$ values.

These two thresholds occur at relatively low values of $C_{CO_2}$. This is useful from a production point of view since saturated conditions do not need to be maintained in the broth at all times, which reduces expensive sparging costs. $CO_2$ utilization most likely limits succinic acid productivity and yield due to the transfer of $CO_2$ across the cell membrane, enzyme activity or gas-liquid mass transfer. It is recommended that the exact limiting mechanism be determined to identify strategies to improve $CO_2$ utilization.

# 6 References

Alibaba (2016). “Dextrose monohydrate”. Available at: http://www.alibaba.com [accessed on 24 January 2016].

Allied Market Research (2014). “World bio succinic acid market – Opportunities and forecasts 2013–2020”. Available at: http://www.alliedmarketresearch.com/bio-succinic-acid-market [accessed on 31 January 2016].

Almqvist, H, Pateraki, C, Alexandri, M, Koutinas, A and Lidén, G (2016). “Succinic acid production by *Actinobacillus succinogenes* from batch fermentation of mixed sugars”. *J. Ind. Microbio.l Biotechnol.* DOI 10.1007/s10295-016-1787-x.

Aresta, M, Dibenedetto, A and Angelini, A (2014). “Catalysis for the valorization of exhaust carbon: From $CO_2$ to chemicals, materials and fuels. Technological use of $CO_2$”. *Chem. Rev.,* 114(3), 1709–1742.

Barnes, EM Jr and Kaback, HR (1971). “Mechanisms of active transport in isolated membrane vesicles. I. The site of energy coupling between D-lactic dehydrogenase and β-galactoside transport in *Escherichia coli* membrane vesicles”. *J. Biol. Chem*., 246, 5518–5522.

Black, SD (1997). “Why has glucose to be autoclaved separately”. Available at: http://www.bio.net/bionet/mm/methods/1997-October/062161.html [accessed on 24 May 2013].

Bozell, JJ and Petersen, GR (2010). “Technology development for the production of biobased products from biorefinery carbohydrates – the US Department of Energy’s ‘Top 10’ revisited”. *Green Chem.,* 12(4), 525–728.

Bradfield, MFA and Nicol, W (2014). “Continuous succinic acid production by *Actinobacillus succinogenes* in a biofilm reactor: Steady-state metabolic flux variation”. *Biochem. Eng. J.,* 85, 1–7.

Bradfield, MFA and Nicol, W (2016). “Continuous succinic acid production from xylose by *Actinobacillus succinogenes*”. *Bioproc. Biosyst. Eng.*, 39, 233–244.

Bradfield, MFA, Mohagheghi, A, Salvachúa, D, Smith, H, Black, BA, Dowe, N, Beckham, GT and Nicol, W (2015). “Continuous succinic acid production by *Actinobacillus succinogenes* on xylose-enriched hydrolysate”. *Biotechnol. Biofuels*, 8, 181.

Brink, HG and Nicol, W (2014). “Succinic acid production with *Actinobacillus succinogenes*: Rate and yield analysis of chemostat and biofilm cultures”. *Microb. Cell Fact.,* 13, 111.

Cherubini, F (2010). “The biorefinery concept: Using biomass instead of oil for producing energy and chemicals”. *Energy. Convers. Manag.,* 51, 1412–1421.

Corona-González, RI, Bories, A, González-Álvarez, V and Pelayo-Ortiz, C (2008). “Kinetic study of succinic acid production by *Actinobacillus succinogenes* ZT-130”, *Process Biochem.,* 43, 1047–1053.

Cussler, E.L (1997). *Diffusion: Mass Transfer in Fluid Systems*, 2nd ed. Cambridge University Press, United Kingdom.

Dym O, Pratt, EA, Ho, C and Eisenberg D (2000). "The crystal structure of D-lactate dehydrogenase, a peripheral membrane respiratory enzyme". *Proc. Natl. Acad. Sci. USA,* 97, 9413–9418.

Guettler, MV, Jain, MK and Rumler, D (1999). "*Actinobacillus succinogenes* sp. Nov., a novel succinic-acid-producing strain from the bovine rumen". *Int. J. Syst. Bacteriol.,* 49, 207–216.

Guettler, M, Jain, M and Soni, B (1998). "Process for making succinic acid, microorganisms for use in the process and methods of obtaining the microorganisms". USA, *US005723322A.*

Gunnarson, IB, Alvarado-Morales, M and Angelidaki, I (2014). "Utilization of $CO_2$ fixating bacterium *Actinobacillus succinogenes* 130Z for simultaneous biogas upgrading and biosuccinic acid production". *Environ. Sci. Technol,* 48, 12464–12468.

ICIS Chemical Business, D (2012). "Chemical industry awaits for bio-succinic acid potential". Available at: http://www.icis.com [accessed on 29 December 2015].

Kent, RL and Eisenberg, M (1976). "Better data for amine treating". *Hydrocarbon Proc.* 55, 87–90.

Kim, M, Kim, NJ, Shang, L, Chang, YK, Lee, YS and Chang, HN (2009). "Continuous production of succinic acid using an external membrane cell recycle system". *J. Microbiol. Biotechnol.* 19(11), 1369–1373.

Lee, PC, Lee, WG, Lee, SY and Chang, HN (2000). "Succinic acid production with reduced by-product formation in the fermentation of *Anaerobiospirillum succiniciproducens* using glycerol as a carbon source". *Biotechnol. Bioeng*., 72(1).

Lee, P, Lee, S, Hong, S and Chang, H (2002). "Isolation and characterization of a new succinic acid-producing bacterium *Mannheimia succiniciproducens* MBEL55E, from bovine rumen". *Appl. Microbiol. Biotechnol*., 58(5), 663–668.

Lin, H, Bennett, GN and San, K (2004). "Fed-batch culture of a metabolically engineered *Escherichia coli* strain designed for high-level succinate production and yield under aerobic conditions". *Biotechnol. Bioeng.,* 90(6), 775–779.

Lin, SKC, Du, C, Koutinas, A, Wang, R and Webb, C (2008). "Substrate and product inhibition kinetics in succinic acid production by *Actinobacillus succinogenes*". *Biochem. Eng. J.,* 41, 128–135.

Lu, SY, Eiteman, MA and Altman, E (2009). "Effect of $CO_2$ on succinate production in dual-phase *Escherichia coli* fermentations". *J. Biotechnol., 143*, 212–223.

Maharaj, K, Bradfield, MFA and Nicol, W (2014). "Succinic acid-producing biofilms of *Actinobacillus succinogenes*: Reproducibility, stability and productivity". *Appl. Microbiol. Biotechnol.,* 98, 7379–7386.

McKinlay, JB, Laivenieks, M, Schindler, BD, McKinlay, AA, Siddaramappa, S, Challacombe, JF, Lowry, SR, Clum, A, Lapidus, AL, Burkhart, KB, Harkins, V and Vieille, C (2009). "A

genomic perspective on the potential of *Actinobacillus succinogenes* for industrial succinate production". *BMC Genomic,* 11, 680.

McKinlay, JB, Vieille, C and Zeikus, JG (2007). "Prospects for a bio-based succinate industry", *Appl. Microbiol. Biotechnol.,* 76, 727–740.

McKinlay, JB, Zeikus, JG and Vieille, C (2005). "Insights into *Actinobacillus succinogenes* fermentative metabolisms in a chemically defined growth medium". *Appl. Environ. Microbiol.,* 71(11), 6651–6656.

Myriant (2016). "Applications". Available at: http://www.myriant.com [accessed on 31 January 2016].

Na, Z (2015). "Maleic anhydride chain – World market overview". Paper presented at the Chemicals Committee Meeting at APIC, 8 May 2015, Seoul, South Korea.

Podkovyrov, SM and Zeikus, JG (1993). "Purification and characterization of phosphoenolpyruvate carboxykinase, a catabolic $CO_2$ fixing enzyme, from *Anaerobiospirillum succiniciproducens*". *J. Gen. Microbiol.,* 139, 223–228.

Reverdia (2015). "Biosuccinium application". Available at: http://www.reverdia.com [accessed on 29 December 2015].

Rischbieter, E, Schumpe, A and Wunder, V (1996). "Gas solubilities in aqueous solutions of organic substances". *J. Chem. Eng. Data,* 41, 809–812.

Samuelov, NS, Lamed, R, Lowe, S and Zeikus, JG (1991). "Influence of $CO_2$-$HCO_3^-$ levels and pH on growth, succinate production and enzyme activities of *Anaerobiospirillum succiniproducens*". *Appl. Environ. Microbiol.*, 57(10), 3013–3019.

Schumpe, A and Deckwer, WD (1979). "Estimation of $O_2$ and $CO_2$ solubilities in fermentation media". *Biotechnol. Bioeng.,* 21, 1075–1078.

Stepan (2012). "Polyester polyols: C.A.S.E". Available at: http://www.stepan.com. [accessed on 23 January 2016].

Trivedi, BC and Culbertson, BM (1982). *Maleic Anhydride*. Springer Science + Business Media, New York.

Urbance, SE, Pometto, AL III, DiSpirito, AA and Demirci, A (2003). "Medium evaluation and plastic composite support ingredient selection for biofilm formation and succinic acid production by *Actinobacillus succinogenes*". *Food Biotechnol.,* 17(1), 53–65.

Urbance, SE, Pometto, AL III, DiSpirito, AA and Denli, Y (2004). "Evaluation of succinic acid continuous and repeat-batch biofilm fermentation by *Actinobacillus succinogenes* using plastic composite support bioreactors". *Appl. Microbiol. Biotechnol.,* 65, 664–670.

Van der Werf, MJ, Guettler, MV, Jain, MK and Zeikus, JG (1997). "Environmental and physiological factors affecting the succinate product ratio during carbohydrate fermentation by *Actinobacillus sp.* 130Z". *Arch. Microbiol.,* 167, 332–342.

Van Heerden, C.D and Nicol, W (2014). “Continuous succinic acid fermentation by *Actinobacillus succinogenes*”. *Biochem. Eng. J.,* 73, 5–11.

Villadsen, J, Nielsen, J and Lidén, G (2011). *Bioreaction Engineering Principles,* 3rd ed. Springer, New York.

Weisenberger, S and Schumpe, A (1996). “Estimation of gas solubilities in salt solutions at temperatures from 273 K to 363 K”. *AIChE J.,* 42, 298–300.

Werpy, T and Petersen, G (2004). “Top value added chemicals from biomass, Vol. 1. Results of screening for potential candidates from sugars and synthesis gas”. National Renewable Energy Lab., Golden, CO, US.

Xi, Y, Chen, K, Li, J, Fang, X, Zheng, X, Sui, S, Jiang, M and Wei, P (2011). “Optimization of culture conditions in $CO_2$ fixation for succinic acid production using *Actinobacillus succinogenes*”. *J. Ind. Microbiol. Biotechnol.,* 38, 1605–1612.

Zeikus, JG, Jain, MK, Elankovan, P (1999). “Biotechnology of succinic acid production and markets for derived industrial products”. *Appl. Microbiol. Biotechnol.,* 51, 545–552.

Zou, W, Zhu, L, Li, H and Tang, Y (2011). “Significance of $CO_2$ donor on the production of succinic acid by *Actinobacillus succinogenes* ATCC 55618”. *Microb. Cell Fact.,* 10, 87–97.

# Appendix A

*Circles denote steady state values used for analyses.

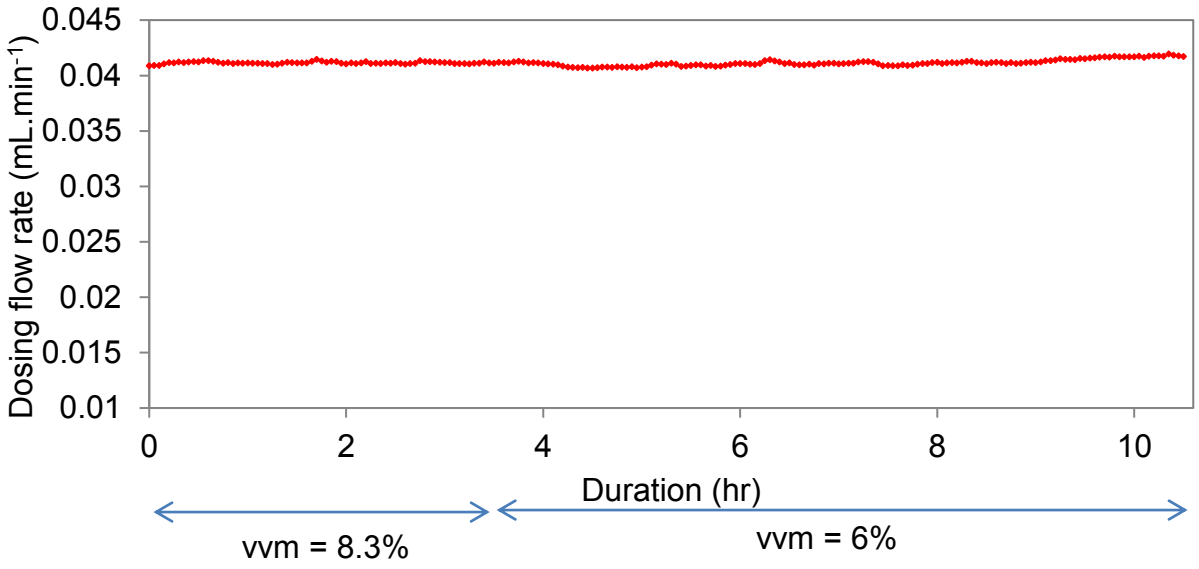


***Figure A-1***: Change in dosing for vvm change from 8.3% to 6%

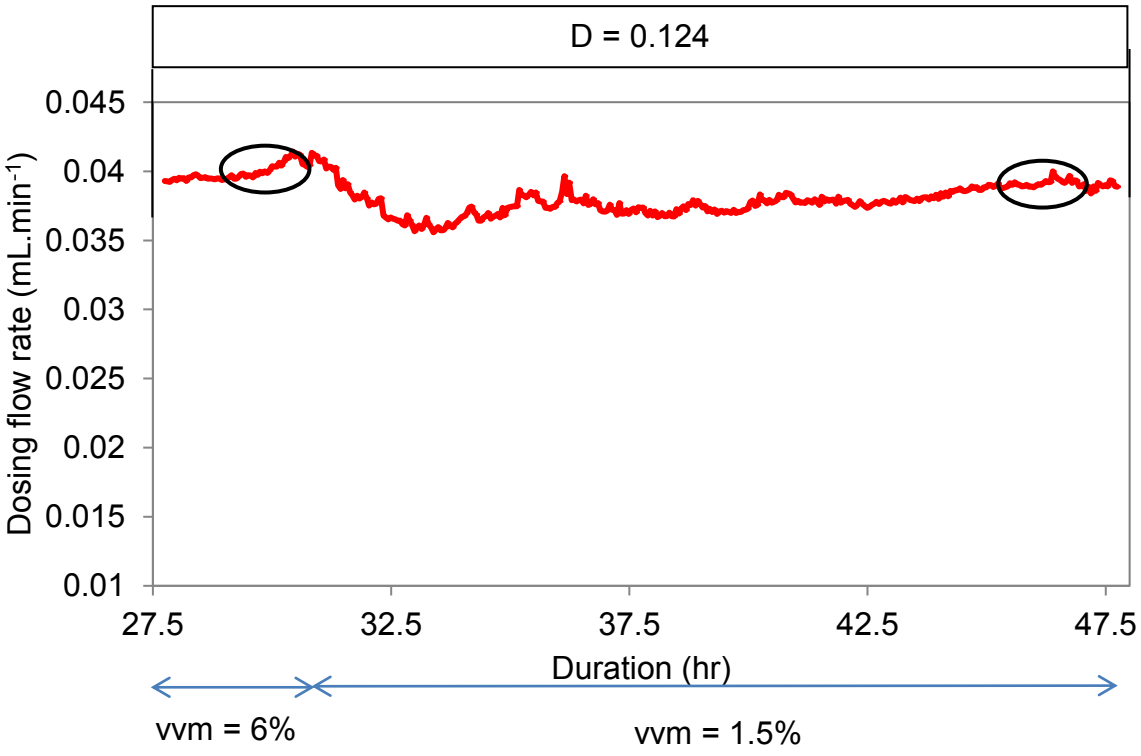


***Figure A-2**: Change in dosing for vvm change from 6% to 1.5%*

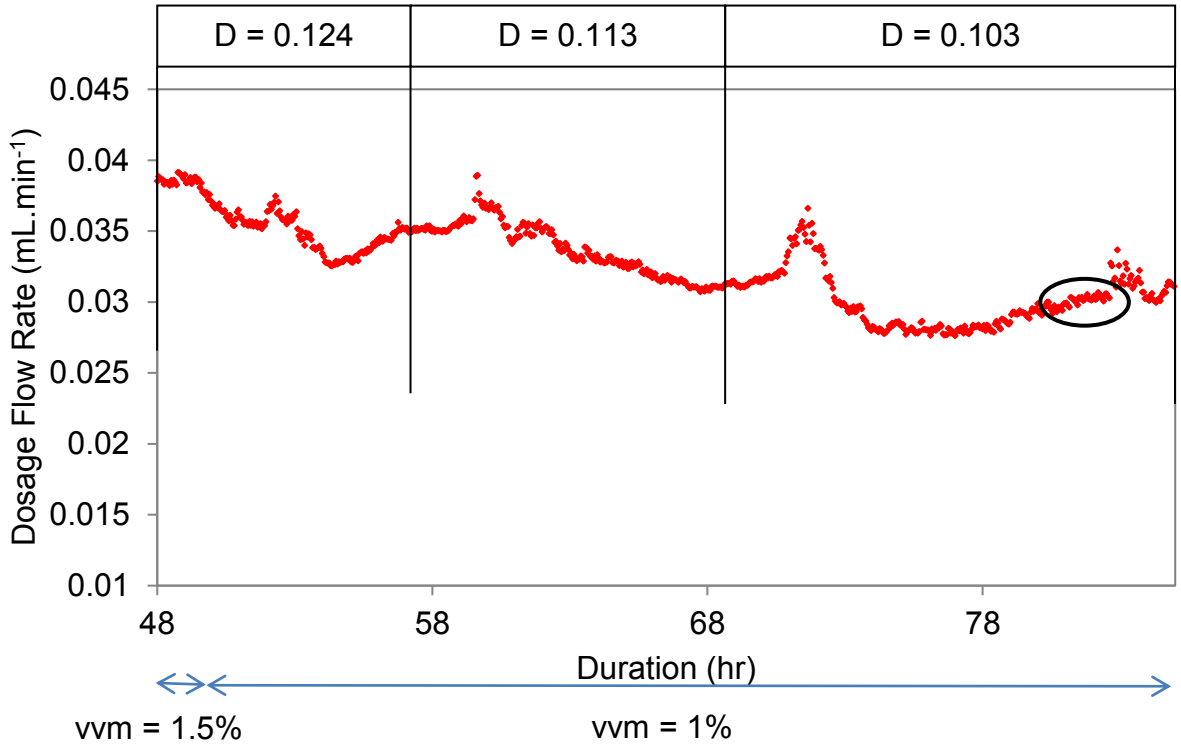


***Figure A-3**: Change in dosing for vvm change from 1.5% to 1%*

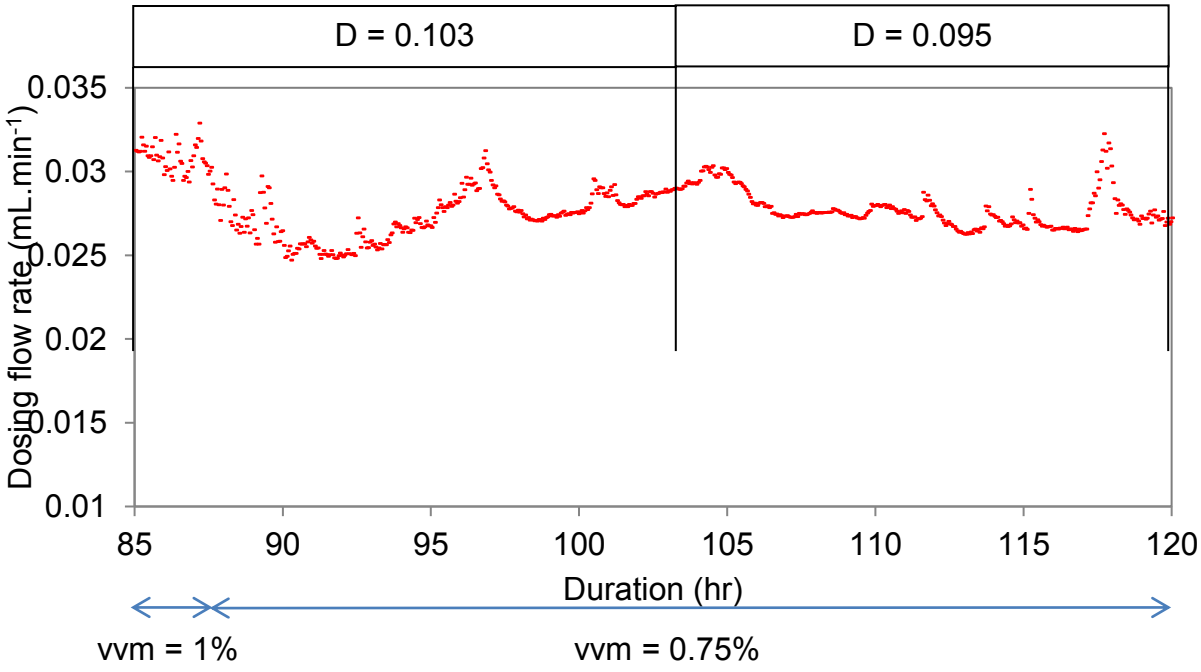


***Figure A-4**: Change in dosing for vvm change from1% to 0.75%*

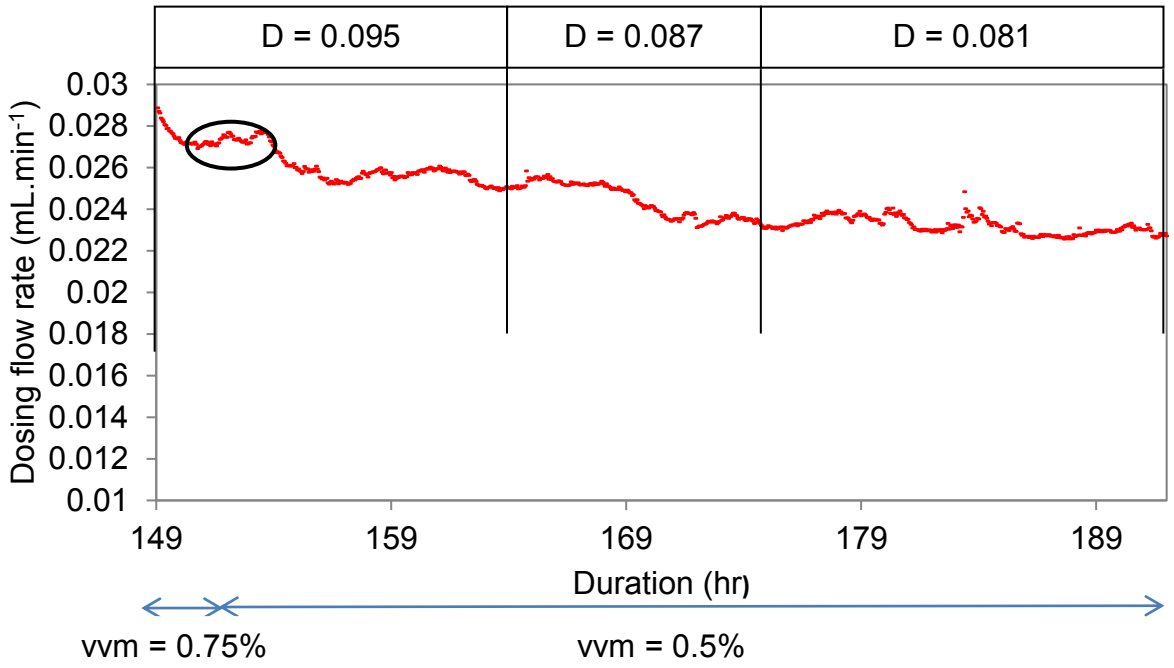


***Figure A-5**: Change in dosing for vvm change from 0.75% to 0.5%*

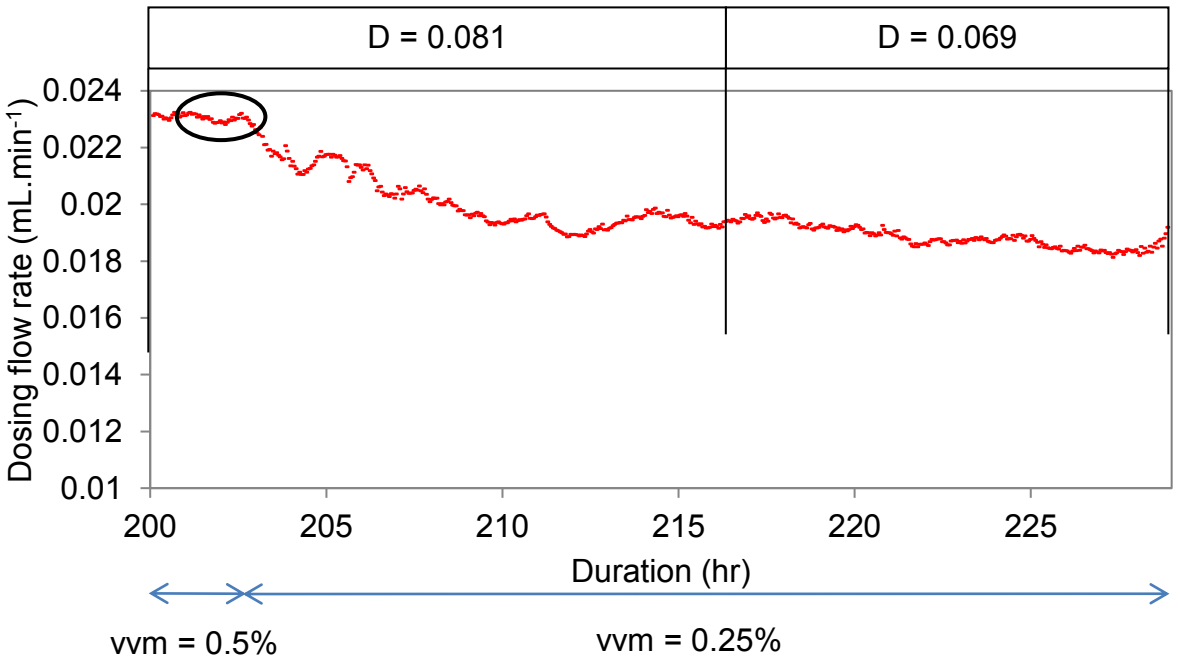


***Figure A-6**: Change in dosing for vvm change from 0.5% to 0.25%*

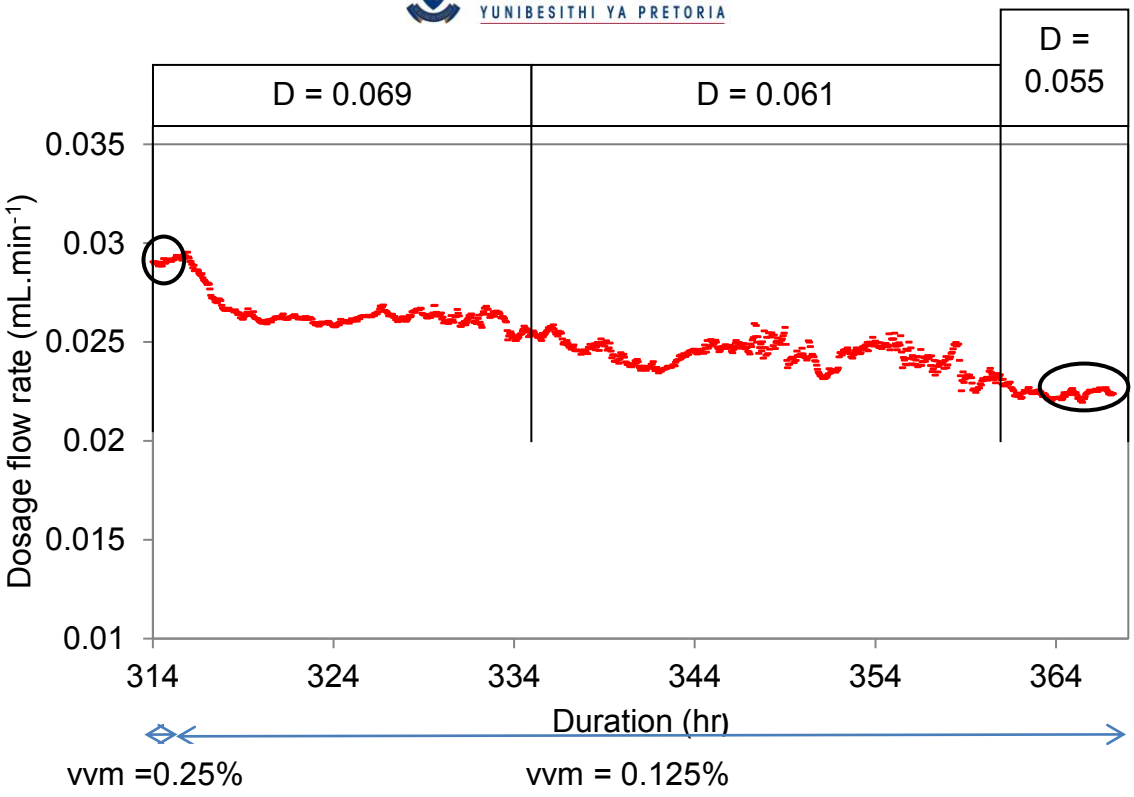


***Figure A-7**: Change in dosing for vvm change from 0.25% to 0.125%*

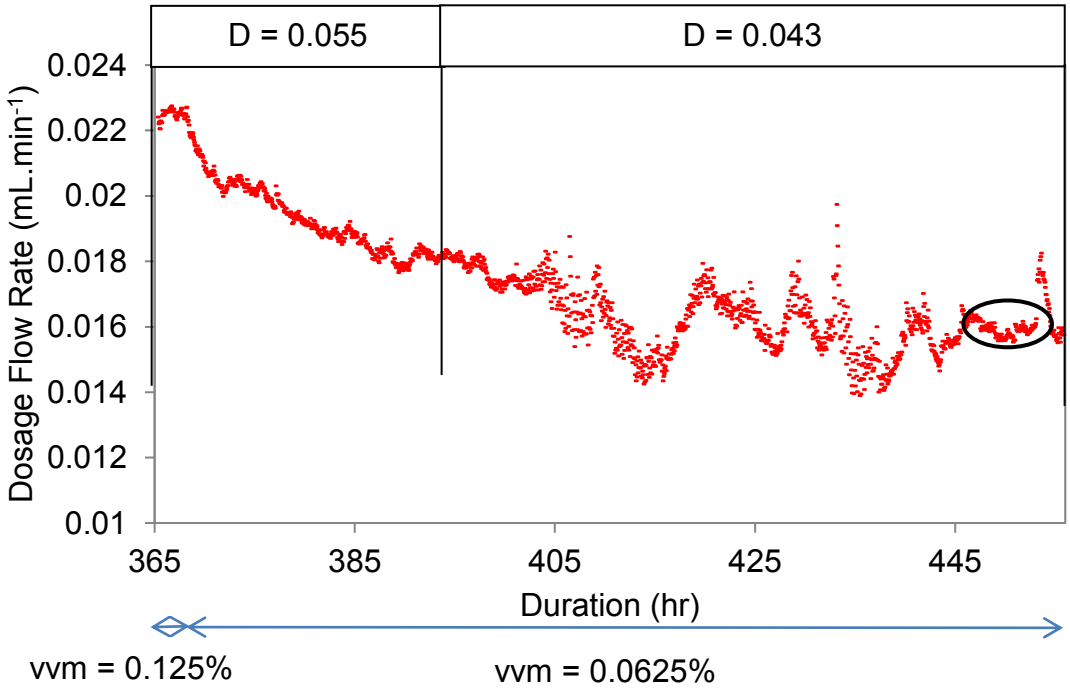


***Figure A-8**: Change in dosing for vvm change from 0.125% to 0.0625%*